Overcoming Undesirable hERG Potency of Chemokine Receptor Antagonists Using Baseline Lipophilicity Relationships

Igor Shamovsky,*,† Stephen Connolly,‡ Laurent David,† Svetlana Ivanova,† Bo Nordén,† Brian Springthorpe,‡ and Klaus Urbahns†

Department of Medicinal Chemistry, AstraZeneca R&D Lund, S-22187 Lund, Sweden, and Department of Medicinal Chemistry, AstraZeneca R&D Charnwood, Loughborough, Leicestershire LE11 5RH, United Kingdom

Received May 9, 2007

The inhibition of the hERG channel by noncardiovascular drugs is a side effect that severely impedes the development of new medications. To increase hERG selectivity of preclinical compounds, we recommend the study of nondesolvation related interactions with the intended target and hERG using a baseline lipophilicity relationship approach. While this approach is conventionally used in studies of potency, we demonstrate here that it can help in selectivity issues. Studies of hERG selectivity in four in-house classes of chemokine receptor (CCR) antagonists suggest that the selectivity is improved most effectively by structural alterations that increase the lipophilicity-adjusted primary potency, $pIC_{50}^{CCR} - \mathrm{Log}D$. Fragment-based QSAR analysis is performed using the lipophilicity-adjusted hERG potency, $pIC_{50}^{hERG} - \mathrm{Log}D$, to identify moieties that form nonhydrophobic interactions with the hERG channel. These moieties, which erode hERG selectivity, can then be avoided. A novel two-dimensional fragment-based QSAR analysis helps visualizing the lipophilicity-adjusted hERG and CCR potencies within chemical series.

Introduction

It is now recognized that some drug-induced sudden deaths are secondary to the development of an arrhythmia called Torsades de Pointes (TdP).[1,2] Recent advances in the understanding of this issue indicate that the primary event is likely to be inhibition of the rapid component of the delayed rectifier potassium current (I_{Kr}) by such agents.[3–5] These compounds bind to the pore-forming α-subunits of the channel protein carrying this current, which are encoded by the human ether-à-go-go related gene (hERG[a]).[1,3,6,7] Because I_{Kr} plays a key role in repolarization of the cardiac action potential, inhibition of potassium efflux via this channel type slows repolarization, which is manifested on the electrocardiogram as a prolongation of the QT interval. While QT interval prolongation is not a safety concern per se, in a small percentage of people it is associated with TdP and degeneration into ventricular fibrillation.

The hERG-encoded channel is blocked by a surprisingly diverse group of drugs, predominantly lipophilic amines.[1,3,6,7] The class III antiarrhythmics and many noncardiovascular drugs in common clinical use prolong the QT interval by this mechanism.[2–5] Evidence of a link to an increased risk of TdP has led to the withdrawal of several drugs from the market (e.g., astemizole, terfenadine, cisapride, sertindole, terodiline, grepafloxacin)[1,3,6–9] and therefore to considerable regulatory sensitivity on this topic.[10] The implications of the clinical guideline (ICH E14) are particularly far-reaching because it requires every drug with systemic bioavailability to be studied in the so-called "Thorough QT/QTc Study", a dedicated ECG study powered to detect an increase in QT interval duration of around 2.5%. Prolonging the QT interval in this study will have a significant impact on the cost of and timelines for drug development and will be likely to limit the commercial value of the product. Understandably, the withdrawal of marketed drugs has led to considerable interest in detecting and predicting compounds with QT liabilities earlier and more efficiently in their discovery timeline.[1,3,4,8,11–19]

To design drugs with a reduced risk of prolonging the QT interval, it would be advantageous to identify and avoid structural features that are beneficial for hERG inhibition. A number of hERG channel pharmacophores have been developed, with the key determinants being a protonated basic nitrogen surrounded by several aromatic or hydrophobic groups.[7,9,12–15,20–23] It has been found that a hydrogen-bond (H-bond) acceptor or an electron-withdrawing atom located at the periphery of the molecule may also contribute to high-affinity binding to hERG.[1,7,17,19,22,24] Based on these studies, a number of lead optimization approaches to avoid hERG blockage have been proposed. These include subtle peripheral structural modifications, removing distal aryl groups, adding an acidic function or its bioisostere, decreasing lipophilicity, decreasing pK_a of the most basic nitrogen, introducing geometric constraints, and changing molecular shape.[3–5,7,9,25–35] Although it has been shown that all of these approaches work in particular cases, none of them is a panacea. The main drawback of these approaches is that, as well as decreasing potency at the hERG channel, they more than often simultaneously decrease the potency at the intended target.[35–38]

Previous efforts to rationalize hERG binding by building 3D hERG pharmacophore models[1,9,12,17,18,20–22,26,39] or defining molecular fragments that cause hERG binding using fragment-based QSAR analysis[14–16] have been based on the overall hERG potency of hERG blockers, pIC_{50}^{hERG}. The conventional routine

* To whom correspondence should be addressed. Telephone: +4646-338347. Fax: +4646-337119. E-mail: igor.shamovsky@astrazeneca.com.
† AstraZeneca R&D Lund.
‡ AstraZeneca R&D Charnwood.

[a] Abbreviations: hERG, human ether-à-go-go-related gene; BLR, baseline lipophilicity relationship; CCR, chemokine receptor; GPCR, G-protein-coupled receptor; QTc, corrected QT interval; ECG, electrocardiogram; H-bond, hydrogen bond; TM7, transmembrane α-helix number 7; OPLS2005, optimized potential for liquid simulations version 2005; RHS, right-hand side; LHS, left-hand side; DSM, discrete structural modifications.

10.1021/jm070543k CCC: $40.75
Published on Web 02/08/2008

of direct use of pIC_{50} values for optimizing potency can be ineffective when one needs to decrease nonspecific hERG binding and at the same time increase or maintain binding to the intended target. The potency of drugs is fundamentally linked to their lipophilicity[40–42] because binding to protein binding sites, which generally represent solvent-exposed hydrophobic surfaces with few polar groups,[43,44] is facilitated by partitioning of hydrophobic drug molecules to these binding sites.[41,45] This equally concerns both intended and off-target binding, therefore, selectivity (the difference in binding affinities) is often independent of compound lipophilicity. Notably, the overall hERG potency of compounds is known to be linked to their lipophilicity, therefore, lipophilic pharmacophore features will inevitably dominate in hERG pharmacophore models.[4,12,20–22,26,39] To decrease binding to hERG, compound lipophilicity cannot be blindly reduced just because hERG potency correlates with lipophilicity, because a certain level is required to maintain permeability and bioavailability and, most importantly, lipophilicity adds to the primary potency of compounds. Although it is common practice in fragment-based QSAR analysis and 3D-QSAR modeling,[4,12,14–16,21,26] it can be deceptive to use direct values of hERG potency in studies aimed in reality at increasing hERG selectivity of compounds. Another questionable practice in fragment-based QSAR studies of hERG selectivity is to directly use the values of hERG potency in mixed sets of compounds aimed at different primary targets. In this case, it is easy to get a simplistic conclusion that, for instance, basic nitrogen should be avoided, whether it is required for the intended target or not.[15,16] Thus, a drawback of the current approaches to address hERG issues of potential drugs is that the need to retain potency at the primary target is not explicitly taken into consideration while attempting to reduce hERG potency.

To develop a successful lead optimization strategy aiming at overcoming hERG-related safety issues, focus should be on hERG selectivity rather than hERG potency alone. In this report, we use the baseline lipophilicity relationship (BLR) approach[40,45–47] to distinguish structural alterations that can increase hERG selectivity from those that tend to affect the potencies at the intended target and at hERG simultaneously. The origin of this approach is the linear correlation between binding affinity and lipophilicity, in the form of either log*P* or log*D* values, that has been experimentally observed in numerous classes of membrane-binding and receptor-mediated drugs since the classical works of Overton and Meyer.[48,49] While the BLR approach has previously been shown to be useful in potency studies, we take this step further and apply it to selectivity issues. Because this approach allows one to remove the desolvation component from the overall hERG potency within chemical series, it opens the possibility for analysis of the purely structural aspects of hERG selectivity.

In this communication we apply the BLR approach to study hERG selectivity of four structurally diverse classes of CCR antagonists that bind to CCR1, CCR3, and CCR8. All compounds were subjected to the same hERG binding assay, avoiding issues with data inhomogeneity. There is a specific reason for focusing on CCR antagonists in studies on hERG selectivity. Chemokine receptors belong to a G-protein-coupled receptor (GPCR) superfamily, and CCR antagonists often contain a basic amine[50] to interact with the TM7 glutamate residue in chemokine receptors,[51] thus displaying a pharmacophore identifiable with common hERG blocking agents. Within the CCR antagonist field, only a few compounds have survived development, and much of this preclinical attrition is due to the challenges of optimizing hERG selectivity.[52–54]

Methods

BLRs of hERG and hERG Selectivity in Chemical Series. BLRs, which express linear correlations between free energy of binding and logarithm of *n*-octanol/water partition coefficient, have become fundamental in drug design.[40,41,45–47,55–58] If potency was due to lipophilicity driven partition alone, a straight line correlation would be observed. However, since factors other than desolvation also contribute to the total binding energy of drugs (that is direct interactions with the binding site, such as van der Waals interactions, H-bonding and π-π interactions), it is typical to find several parallel lines in the leading edge of potency/lipophilicity plots of structurally diverse compound sets.[40,45–47,55,59,60] Where compounds fall off the leading edge, it is likely due to the added component disrupting geometric fit to the binding site. Each of these lines represents a subset of closely related structural analogues, for which such direct interactions are similar,[42,45,47,55,59,60] but the measured potency varies with the nonspecific lipophilicity-driven binding component. The slope of the lines is related to the extent of hydrophobic amino acids lining the binding site pocket, and is called the hydrophobicity factor of the binding site.[45,47,60] The value of the slope usually varies from 0.3 to 1.3, being most of the time around 1.[40,42,43,60] In other words, the gain in potency (ΔpIC_{50}) within a closely related subset of compounds is often observed to be roughly equal or at least proportional to the added lipophilicity ($\Delta \log P$),[40–43,45–49,55–57,59–61] while being insensitive to the particular structural elements that cause these changes in lipophilicity.[40–47,61–64]

Mathematically, the BLR[45–47] represents a split of Gibbs energy of binding (ΔG) into two components, namely, free energy of partitioning of a molecule to an organic phase and free energy of nonhydrophobic interactions taking place between the counterparts in the bound complex. This relationship can be expressed as a link between lipophilicity (log*D*) and potency (pIC_{50}) of drugs:[40,45–47,60]

$$pIC_{50} = a \times \log D - k \times \Delta G_{intr} + \text{const} \qquad (1)$$

where pIC_{50} is the potency of a compound; *D* is the apparent *n*-octanol/water partition coefficient; *a* is the hydrophobicity factor of the binding site; *k* is a coefficient equal to $(2.303 \times RT)^{-1}$; and ΔG_{intr} is the intrinsic binding energy, which is not related to desolvation and describes polar interactions and geometric fit in the bound complex.

The first term of eq 1 ($a \times \log D$) is the lipophilicity driven component of potency caused by desolvation. The values of log*D*, rather than log*P*, are utilized to quantify the lipophilicity of ionized compounds, primarily because log*D* is an experimentally derived property. The log*D* value is a function of the partitioning of the neutral form of the compound (log*P*) and its ionization degree at pH 7.4, which may somewhat complicate comparisons of measured lipophilicities of compounds of different ionization types.[25] The second term ($-k \times \Delta G_{intr}$) is the intrinsic potency, which is not related to desolvation. It results primarily from direct interactions of the bound drug with the binding site, consisting of polar interactions, such as H-bonds and salt bridges, but also $\pi-\pi$, cation$-\pi$, hydrophobic packing, and van der Waals interactions. In cases of partial desolvation of ligands in bound complexes, the second term also includes the solvation energy of solvent-exposed moieties.

Values of the hydrophobicity factors of binding sites in eq 1 are determined by regression analysis by considering only

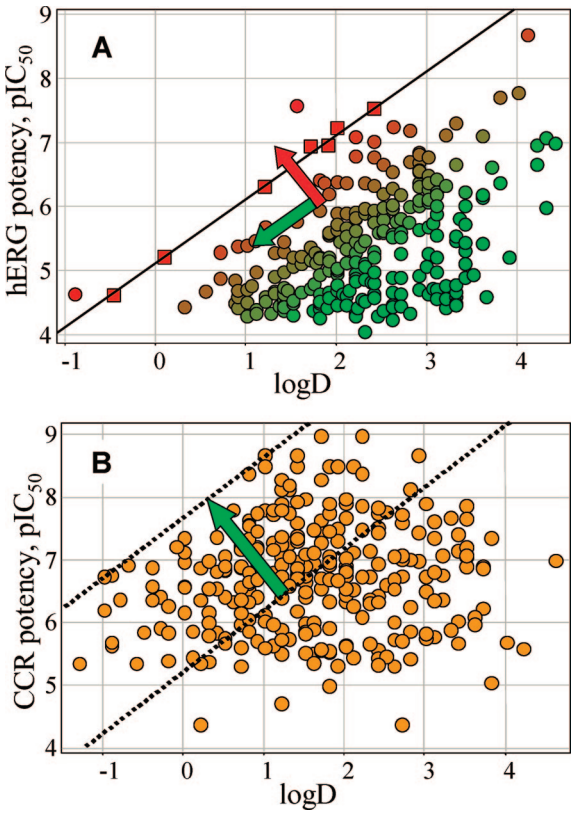

Figure 1. Graphical interpretation of the strategy to improve hERG selectivity of CCR antagonists. (A) Typical potency/lipophilicity plot for inhibitors of the hERG channel. The straight line with the slope of a^{hERG} is the line of the best fit for the structurally closely related subset of compounds (datapoints given in squares). The color of datapoints indicate intrinsic hERG potency (red for high, green for low). (B) Typical potency/lipophilicity plot for the primary target. The diagonal line of the same slope is described by eq 3. To improve hERG selectivity, one has to make structural alterations that move the corresponding datapoints in the directions shown by the green arrows in plot A, $-pIC_{50}{}^{hERG} - (a^{hERG})^{-1} \times \log D$, and plot B, $pIC_{50}{}^{CCR} - a^{hERG} \times \log D$. The red arrow in plot A points to the forbidden direction, $pIC_{50}{}^{hERG} - a^{hERG} \times \log D$, which is a hallmark of direct attractive interactions with the hERG channel.

closely related molecules characterized by similar contributions of intrinsic interactions.[40,45–47,60] A typical potency/lipophilicity plot for a series of hERG channel blockers with the hERG lipophilicity baseline is illustrated in Figure 1A. Using eq 1, the hERG selectivity of CCR antagonists can be written as

$$pIC_{50}{}^{CCR} - pIC_{50}{}^{hERG} = (pIC_{50}{}^{CCR} - a^{hERG} \times \log D) + k \times \Delta G_{intr}{}^{hERG} + \text{const.} \quad (2)$$

The first term in the right side of this expression ($pIC_{50}{}^{CCR} - a^{hERG} \times \log D$) is independent of the binding affinity at hERG. The second term, $k \times \Delta G_{intr}{}^{hERG}$, is the inverse intrinsic potency at hERG, which is independent of binding to the primary target. Our lead optimization strategy is to increase both these terms. Let us set the first term to a constant.

$$pIC_{50}{}^{CCR} - a^{hERG} \times \log D = \text{const.} \quad (3)$$

The graphical representation of eq 3 is a diagonal line in the potency/lipophilicity plot for the primary target (Figure 1B). Note that the slopes of the diagonal lines in Figure 1A,B are identical and equal to the hERG hydrophobicity factor. The increase of the lipophilicity-adjusted primary potency (the first term of eq 2) corresponds to the shift of the diagonal line in the primary target plot to the upper left quadrant (shown by the green arrow in Figure 1B). This means that structural alterations have to lead to increasing or at least retaining the value of $pIC_{50}{}^{CCR}$ by decreasing compound lipophilicity. *Thus, the most important part of increasing hERG selectivity in the chemical series is reducing the desolvation component of the intended potency of compounds and attaining the required potency utilizing direct attractive interactions with the designated binding site.* In case of partial ligand desolvation in the bound complex, the same effect can be achieved by increasing polarity of the solvent-accessible moiety of the ligand. To keep the second term of eq 2 constant while decreasing compound lipophilicity, one has to avoid forming new direct attractive interactions with the hERG channel and thus move lead optimization in the direction shown by the green arrow in Figure 1A. This direction is defined by retaining the value of the lipophilicity-adjusted hERG potency (see eq 1). Intrinsic hERG binding motifs, that is, molecular fragments, which increase the lipophilicity-adjusted hERG potency and thereby move lead optimization in the wrong direction (Figure 1A), have to be avoided. *The second important part of increasing hERG selectivity is to avoid direct attractive polar interactions with the hERG binding site.*

Fragment-Based QSAR Analysis along the Nondesolvation Components of Potency. Fragment-based QSAR analysis performed in the direction of ($pIC_{50}{}^{hERG} - a^{hERG} \times \log D$) in a given chemical series will rank molecular fragments of the common scaffold according to their contributions to the intrinsic hERG potency (eq 1). In addition, this routine will allow one to estimate inherent propensities of different scaffolds for the nondesolvation interactions with the hERG channel. This one-dimensional approach would however overlook the role of the intended potency in hERG selectivity (eq 2). We recommend performing QSAR analysis that would simultaneously take both terms of eq 2 into consideration. Instead of solving the Free-Wilson regression[65] in one direction, we utilized the following two-dimensional fragment-based QSAR analysis. Contributions of each molecular fragment to the left side of eq 2, $Y = (pIC_{50}{}^{CCR} - pIC_{50}{}^{hERG})$, and to the first term of the right side, $X = (pIC_{50}{}^{CCR} - a^{hERG} \times \log D)$, were calculated independently using Free-Wilson regressions,[65] and the obtained values were plotted against each other, as shown in Figure 2. The average values of ΔX and ΔY were set to zero for each attachment point of the scaffolds. This assumption allowed us to estimate the contributions of the scaffolds to X and Y. It can be shown that the direction of $(X - Y)$ is the intrinsic hERG potency (Figure 2).

The new type of two-dimensional fragment-based QSAR analysis allows one not only to detect intrinsic hERG binding fragments within each chemical class, but also to study the effects of direct interactions with the primary target on hERG selectivity. The diagonal line $\Delta X = \Delta Y$ signifies the average contribution of molecular fragments of the particular chemical class to the intrinsic hERG potency. The deviation from this line to the lower right quadrant of the plot indicates productive polar interactions with the hERG channel, as shown by the thick arrow in Figure 2. The corresponding structural motifs responsible for the decrease in the second term of eq 2 are intrinsic hERG binding fragments. Any deviation from this line in the opposite direction is an indication of steric or electrostatic repulsion within the hERG cavity. This is a hallmark of intrinsic hERG nonbinding fragments, which are beneficial for the hERG selectivity. Thus, this straight line separates intrinsic hERG binding from intrinsic hERG nonbinding fragments, and can

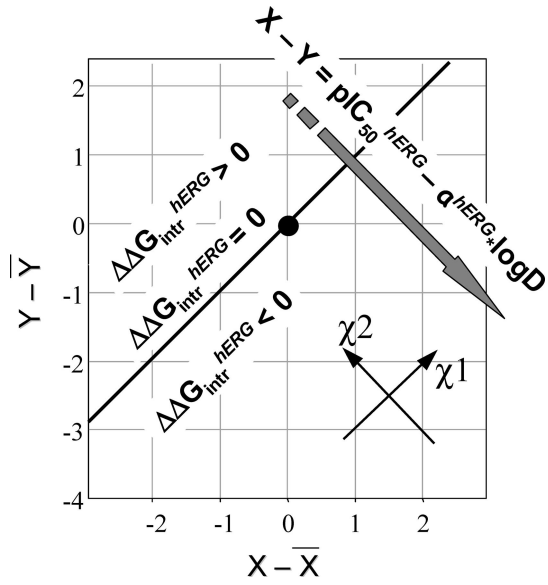

Figure 2. Detection of intrinsic hERG binding and intrinsic hERG nonbinding fragments is performed by plot of relative contributions of different fragments of hERG blockers to $Y = pIC_{50}^{CCR} - pIC_{50}^{hERG}$ and $X = pIC_{50}^{CCR} - a^{hERG} \times \log D$ calculated by fragment-based QSAR analysis. Both variables are centered. The black spot shows the coordinate origin. The diagonal line $X = Y$ is the average hERG lipophilicity baseline separating intrinsic hERG binding and intrinsic hERG nonbinding fragments. The thick arrow, which is perpendicular to this line and points to the direction of $X-Y$, is the nondesolvation component of hERG potency. The new coordinate system ($\chi1 = X + Y$, $\chi2 = Y - X$) allows interpretation of the nature of the increase of hERG selectivity within chemical series. Changes along the coordinates $\chi1$ and $\chi2$ reflect the increases of the first and the second terms of the right side of eq 2, respectively.

be called the average hERG lipophilicity baseline for fragments of the particular chemical class. The new coordinate system ($\chi1$,$\chi2$), which is obtained by the 45° rotation of the original axes X and Y (Figure 2), allows one to study contributions of each structural alteration to the first (axis $\chi1$) and to the second (axis $\chi2$) terms of eq 2. To overcome hERG potency in chemical series, progress in both directions is required.

Pharmacophore Modeling of hERG Blockers along the Nondesolvation Component of hERG Potency. Our experience in optimization of lipophilic amines in several series of CCR antagonists indicates that addition of a wide variety of lipophilic groups in various positions in a molecule will usually result in increased hERG binding. It appears that it is not helpful to think in terms of the optimal positions of hydrophobic features in hERG pharmacophores because they are too elusive and abundant,[22,66] and an altogether different approach to consider hydrophobic interactions with hERG is needed. The set of active compounds to build a pharmacophore for direct nonhydrophobic interactions with the binding site must include structures that exhibit the highest magnitudes of the nondesolvation component of potency, $pIC_{50} - a \times \log D$, rather than the overall potency. Hydrophobic compounds that gain potency mostly by high desolvation energy instead of direct interactions with the binding site have to be excluded. In addition, this pharmacophore type has to account only for attractive polar interactions involving H-bond donors, H-bond acceptors, positive and negative charges, and in special cases, even aryl groups forming $\pi-\pi$ interactions, as well as for spatial hindrances obstructing geometric fit. Hydrophobic pharmacophore features should be explicitly excluded.

Pharmacophore modeling of intrinsic hERG binders was performed using the program Phase (Schrödinger, New York, NY, U.S.A.). Each molecule taken in its protonation state at pH = 7.4 was represented by a set of low-energy conformers generated by MacroModel (Schrödinger, New York, NY, U.S.A.) with the "Ligand torsion search" engine using the OPLS2005 force field (Schrödinger, New York, NY, U.S.A.) with the Generalized Born solvent model.[67] Conformational spaces of piperidine rings were not sampled in order to avoid twisted conformations.

Homology Modeling of hERG. The homology model of the tetrameric pore domain of the hERG channel was built by the program Modeller/InsightII (Accelrys, San Diego, CA, U.S.A.) using a 1.9 Å resolution X-ray structure of the KcsA potassium ion channel crystallized in a closed state as a template from the PDB entry 1R3J.[68] The positions of critical segments in the hERG channel sequence, that is, transmembrane helices S5 and S6, pore helix P, and the selectivity filter SF, and alignment with the KcsA channel were used as previously described.[11,24] The 22-residue region of the hERG sequence encoding the extracellular "turret" helix of hERG was omitted.[3,24,66] The choice of this particular template being in the closed, rather than open, state was made for the following reasons. It was shown that inactivation of the hERG channel results in increased drug binding,[3,69] therefore, it was assumed that, although drugs enter the internal mouth of the hERG channel in its open state,[13,70] inactivation is likely to entrap them and optimally position all residues involved in drug binding.[66,71,72] If the open state of the voltage-dependent KvAP potassium ion channel[73] is utilized as a template for homology modeling, the cytosolic ends of the S6 helices of the resulting hERG channel model are moved away from the channel axis,[24] which makes it difficult to explain the demonstrated importance of residue V659 for binding of a number of hERG blockers.[3,19,66] On the other hand, in the homology model derived from the structure of the closed channel KcsA, the inner S6 helices of the channel come too close to each other in the area of the intracellular opening, which makes the central cavity and residues V659 inaccessible for interactions with hERG blockers (Figure 3A).[66] In a way the open state channel appears to be too wide, but the closed state is too obstructed. Because the purpose of the homology modeling was to understand the key 3D elements of high affinity hERG binding, we used the closed hERG model as the starting point and "opened" the central cavity of the channel by energy refinements with an enclosed hERG blocker.[66]

The hERG blocker terfenadine in its protonated state was placed along the 4-fold hERG channel axis in the closed model of the hERG channel, such that the bulky diphenylmethanol moiety is located inside the wide inner cavity. A putative 3D structure of the terfenadine-hERG complex was obtained by empirical force field potential energy minimization using the program Sybyl (Tripos, St. Louis, MO, U.S.A.) and the MMFF94s force field. The geometry and position of terfenadine and the inner transmembrane helix S6 were optimized in the gas phase using a distance-dependent dielectric constant. Backbone dihedral angles within S6, together with the 3D structure of the backbone of the rest of the channel, except for G648, were maintained unchanged. Residue G648 is conserved within the K^+ channel family and is thought to be a K^+ channel glycine hinge, a point of flexibility that permits channel opening.[66,74,75] As a result of the energy minimization, the internal mouth of the channel was opened as illustrated in Figure 3.

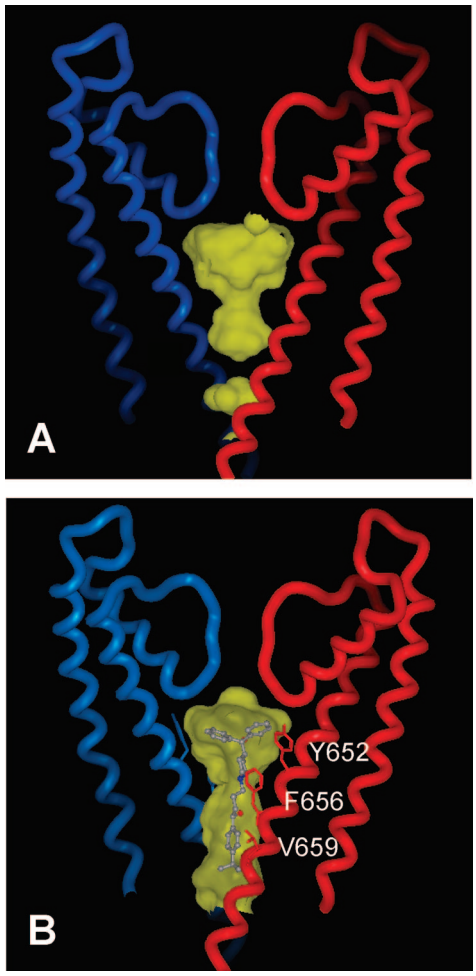

Figure 3. A putative model of the pore domain of hERG channel with bound terfenadine. (A) Preliminary model obtained by homology modeling using the X-ray structure of KcsA as a template. (B) The refined model after energy minimization with the enclosed ligand. Two out of four subunits comprising the tetrameric channel are illustrated. Side chains of the S6 helix residues that were identified as critical for high affinity binding of hERG blockers are shown in (B). The surface of the hERG channel vestibule is depicted yellow.

Docking of Intrinsic hERG Binders to the hERG Homology Model. The purpose of the docking exercise was to find possible explanations for the observed intrinsic hERG binding. Putative binding modes of extreme cases of intrinsic hERG binders in the hERG ion channel were obtained in three steps. An initial binding mode of a chosen hERG inhibitor taken at its protonation state at pH = 7.4 was predicted by the program Glide (Schrödinger, New York, NY, U.S.A.) in the extra precision mode XP.[76,77] No potassium ions were loaded to the selectivity filter in the docking calculations, as their presence does not affect the docking results.[24] Multiple molecular dynamics runs for 50 ps at constant temperature of 300 K were subsequently performed by the program MacroModel using the OPLS2005 force field and the generalized Born solvent model, which were followed by local minimum energy refinements. Molecular dynamics simulations and energy minimization steps allowed conformational changes in the ligand and in the side chains of all hERG channel residues. The structure corresponding to the minimum of potential energy was chosen for each complex.

Results and Discussion

Test Chemical Classes. The BLR approach and the two-dimensional fragment-based QSAR analysis have been applied to four in-house chemical classes targeting three chemokine receptors, CCR1, CCR3, and CCR8, to devise general rules of overcoming hERG related issues. While the hERG-binding propensity is a property of the whole molecule, the fragment-based QSAR analysis ranks their fragments, which can be common for molecules belonging to different chemical classes and different primary targets, therefore it is important to see whether the rules are scaffold- or target-independent. General structures of the CCR antagonists under consideration are presented in Figure 4.[78–81] The four classes **I**−**IV** included 42, 110, 138, and 82 compounds, respectively. The logarithm of the apparent *n*-octanol/water partition coefficient, Log$D_{7.4}$, potency of binding to the corresponding primary target, pIC_{50}^{CCR}, and potency of binding to hERG ion channel, pIC_{50}^{hERG}, have been experimentally determined for these compounds as described in the Experimental Section.

The hERG BLRs. Figure 5 illustrates hERG potency/lipophilicity plots for the test classes. The straight line fit is performed independently in each of these classes using structurally closely related analogues. Scaffolds of the chosen subsets are given in Figure 6. A proper choice of the subsets of hERG blockers is particularly important because of the promiscuous nature of the channel for drug interactions.[82] To form the subsets, we used the following five criteria, which are in line with common practice.[40,45–47] First, the subset has to be close to the leading edge of the hERG potency/lipophilicity plot of the particular chemical class, such that productive polar interactions with the binding site in the subset are exemplified. Second, steric locations of key polar functional groups that are critical for hERG binding have to be the same within the subset. Third, the subset has to be sufficiently populated and contain at least six compounds. Fourth, standard errors of the estimates have to be reasonable (not higher than 20%). Fifth, several independent evaluations of the hydrophobicity factor of the binding site using different chemical classes are necessary.

The estimates of the hERG binding site hydrophobicity factor (a^{hERG}), obtained by regression analyses of eq 1 using limited subsets of compounds, are 0.93 ± 0.17 (n = 11), 1.26 ± 0.12 (n = 8), 0.85 ± 0.12 (n = 15), and 0.95 ± 0.16 (n = 16) for classes **I**−**IV**, respectively. This suggests that the hydrophobicity factor of hERG binding site (a^{hERG}) for different classes of CCR antagonists is close to 1.0, which means that the increase of lipophilicity by one log unit results in a rise in hERG potency also by about one log unit, within closely related subsets. Interestingly, the overall effective hydrophobicity factor of the hERG channel for binding of a wide variety of ligands has been recently estimated to be around 0.8.[9] The value of the hydrophobicity factor is a measure of the desolvation related interactions with the binding site, and as such has to be distinguished from the overall effect of compound lipophilicity on potency. When considering a wide variety of ligands, compounds in the polar end of the overall lipophilicity range may form specific polar interactions with the binding site, which makes them more potent than it would be expected according to their polarity.[1,7,17,19,22,24,41] At the same time, lipophilic compounds may carry bulky lipophilic motifs that most commonly do not fit to the binding site cavity, which makes them less potent than expected according to their lipophilicity.[9,83–86] These effects may result in an underestimation of the actual desolvation effects in hERG potency when using structurally diverse sets of ligands.

The importance of taking BLRs into account in lead optimization is illustrated by statistical considerations presented in Table 1. The correlation coefficients are calculated separately

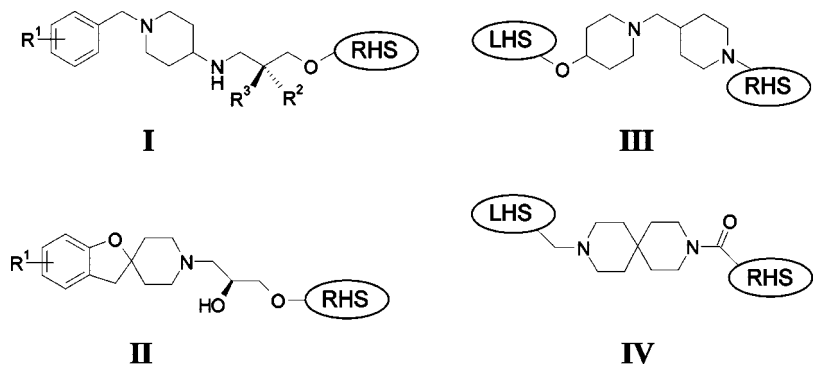

Figure 4. Core structures of four classes of chemokine receptor antagonists. LHS and RHS designate hydrophobic left-hand-side and polar right-hand-side moieties, respectively; R^1, R^2, and R^3 are small functional groups.

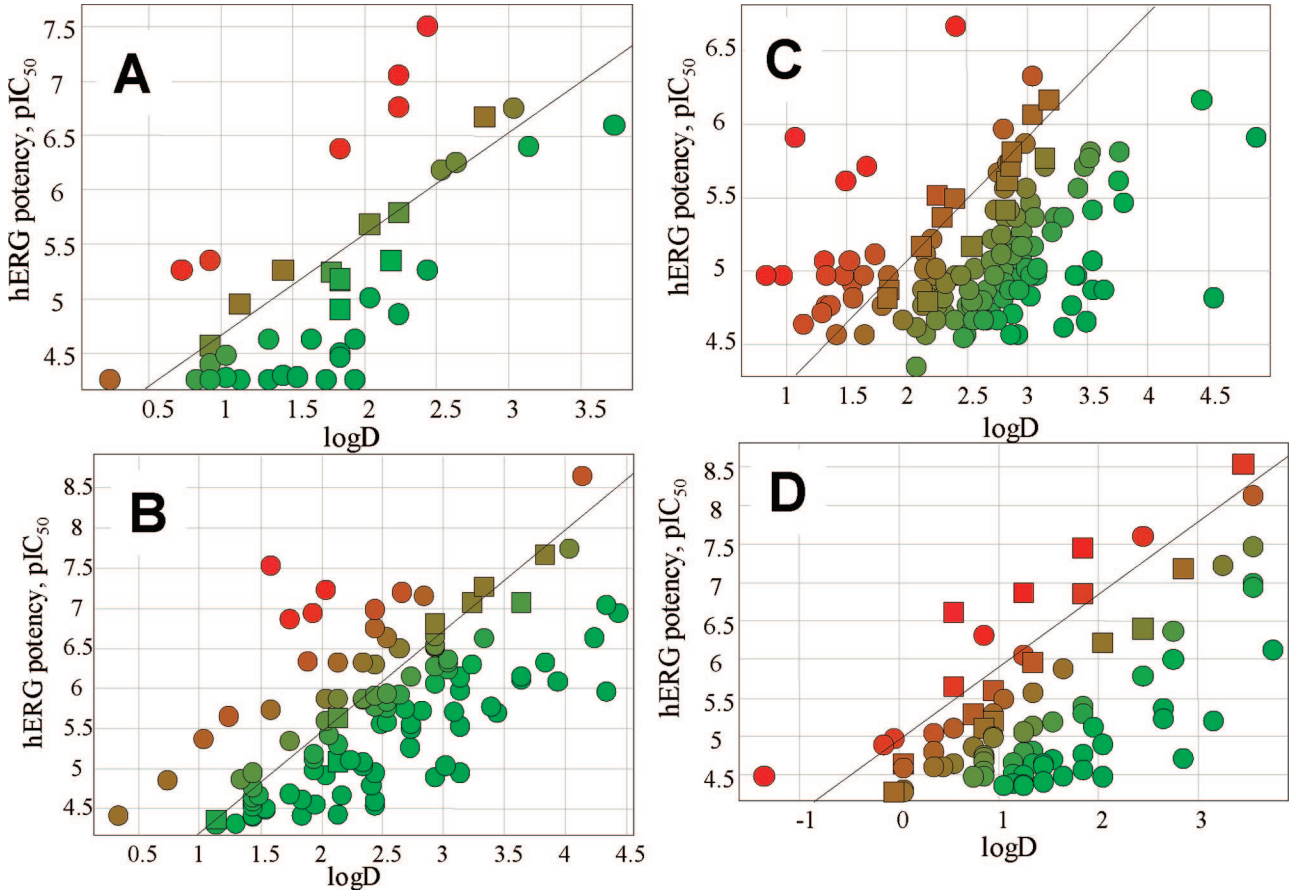

Figure 5. Plots of hERG binding potency versus lipophilicity for compounds of the considered classes. (A) **I**; (B) **II**; (C) **III**; (D) **IV**. The straight lines are determined by regression analyses using close homologues indicated by squares. The slopes of the lines represent estimations of the hERG binding site hydrophobicity factor a^{hERG}. Color of circles designates intrinsic hERG potency, which alters from intrinsic hERG nonbinders (green) to intrinsic hERG binders (red).

for each of the four test series. Results indicate that correlation of hERG potency with compound lipophilicity is significantly more pronounced than correlation of hERG selectivity with compound lipophilicity. This confirms our assumption that the lipophilicity driven component of hERG potency of chemokine receptor antagonists gets significantly reduced in the hERG selectivity expression by a similar component of the primary potency, which suggests that it is problematic to improve hERG selectivity by decreasing compound lipophilicity. Consistent with eq 2, data also indicate that improvement of hERG selectivity within all the considered structural classes is achieved more efficiently by increasing the value of the lipophilicity-adjusted primary potency ($\mathrm{pIC_{50}}^{\mathrm{CCR}} - a^{\mathrm{hERG}} \times \log D$) than by decreasing hERG potency or its components. It should be noted, however, that the approach to decrease hERG potency is as effective in increasing hERG selectivity in classes **III** and **IV**. This statistical analysis supports the theory that a "one-dimensional" approach for solving selectivity issues based purely on compound lipophilicity or hERG potency is likely to be less effective than the "two-dimensional" approach to increase the nondesolvation related component of the primary potency. The latter approach will be even more efficient if molecular fragments that form attractive intrinsic interactions with the hERG channel are detected in the course of lead optimization and avoided.

Detection of Molecular Motifs with High hERG-Binding Propensities. Contributions of scaffolds and molecular motifs to the intrinsic hERG potency are evaluated by the fragment-based

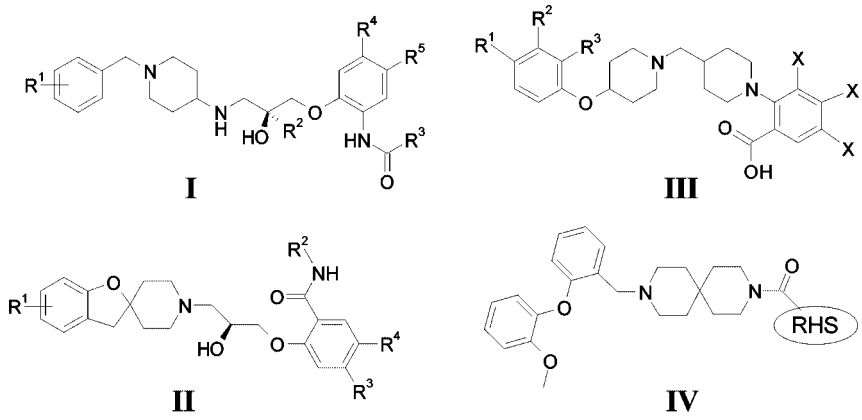

Figure 6. Scaffolds of closely related subsets of the structural classes, which are used to evaluate the hydrophobicity factor of the hERG binding site. X designates H, F, or Cl; R^i designates a small substituent.

Table 1. Correlation Coefficients (R) between Variables X1 and X2 Calculated Using Measured Values of the Test Series (Classes **I**−**IV**)[a]

X1	X2	I	II	III	IV
pIC_{50}^{hERG}	log$D$	0.72	0.64	0.35	0.64
$pIC_{50}^{CCR} - pIC_{50}^{hERG}$	log$D$	−0.53	−0.42	0.094	−0.43
$pIC_{50}^{CCR} - pIC_{50}^{hERG}$	pIC_{50}^{hERG}	−0.74	−0.66	−0.60	−0.75
$pIC_{50}^{CCR} - pIC_{50}^{hERG}$	$pIC_{50}^{hERG} + \log D$	−0.69	−0.61	−0.20	−0.65
$pIC_{50}^{CCR} - pIC_{50}^{hERG}$	$pIC_{50}^{hERG} - \log D$	−0.47	−0.35	−0.48	−0.36
$pIC_{50}^{CCR} - pIC_{50}^{hERG}$	$pIC_{50}^{CCR} - \log D$	**0.85**	**0.82**	**0.62**	**0.76**

[a] The value of hERG selectivity ($pIC_{50}^{CCR} - pIC_{50}^{hERG}$) increases more reliably within each class when increasing the value of ($pIC_{50}^{CCR} - \log D$) of compounds, than by decreasing their lipophilicity (log$D$), hERG potency (pIC_{50}^{hERG}), the desolvation component of hERG potency ($pIC_{50}^{hERG} + \log D$), or nondesolvation component of hERG potency ($pIC_{50}^{hERG} - \log D$), as illustrated by the underlined maximal values of correlation coefficients.

QSAR analysis for the four test series. Scaffolds of classes **I**−**IV** add to the intrinsic hERG potency as much as 3.80, 3.37, 2.58, and 4.00 log units, respectively. These estimates indicate that different scaffolds exhibit quite different potentials for overcoming hERG related issues in lead optimization, with the scaffolds of the classes **III** and **IV** being the most and the least promising, respectively. Class **IV** displays an inherent predisposition for hERG binding, such that it might be problematic to achieve the required balance of hERG selectivity and compound lipophilicity, unless intrinsic hERG nonbinding motifs are found.

Figure 7 illustrates the results of the two-dimensional QSAR analysis, which allow the detection of intrinsic hERG binding structural motifs in the compounds of the considered classes. These plots also reveal the role each fragment plays in hERG selectivity of compounds. It can be noticed that the majority of the structural motifs of CCR antagonists studied are located in the vicinity of the average hERG lipophilicity baselines, which indicates that their role in improving hERG selectivity is to form nondesolvation related interactions with the primary target. Nevertheless, there are a great number of outliers below the baselines, which represent intrinsic hERG binding fragments working against the hERG selectivity. Because the plots are derived from experimentally measured values, which are subject to errors, we have to estimate the magnitude of the smallest deviation from the baseline that would be beyond experimental errors. By assuming realistic standard errors in measuring values of pIC_{50} to be around 0.3 (which corresponds to a 2-fold difference between independent measurements of IC_{50} values), we define the smallest significant deviation from the baseline to be one log unit. Accordingly, we find that 32 out of 298 fragments (i.e., 11%) in the four structural classes can be regarded as intrinsic hERG binding fragments. These fragments contribute to hERG potency at least 10 times more than an average molecular fragment of the same lipophilicity attached to the same place of the same scaffold. The maximal detected deviation from the average hERG lipophilicity baseline induced by a single molecular fragment is found in class **II** and is as high as 440 times. The percentage of intrinsic hERG binding fragments may not seem high until we bear in mind that the increased hERG potency associated with these fragments is absolutely unintentional, *which demonstrates a surprising potential for attractive intrinsic polar interactions in the hERG channel cavity*.

The plots shown in Figure 7 reveal that specific structural elements in the polar RHS moieties are mainly responsible for the increase of the intrinsic primary potency, and equivalent improvement of hERG selectivity of compounds in classes **I**, **II**, and **III**. However, at the same time, it is also specific structural elements in the polar RHS fragments, though subtly different ones, that give rise to most of intrinsic hERG binding moieties. Results indicate that effects of structural changes in R^1, R^2, and R^3 in class **I** are minor; correspondingly, no functionalities at these positions contribute significantly to intrinsic hERG binding. Effects of changes in R^1 in class **II** are more pronounced, but the locations of the corresponding datapoints close to the average hERG lipophilicity baseline indicate that they do not differ in intrinsic hERG binding. Only one fragment was identified at the LHS in class **III** compounds as adding an unusually high value to the hERG binding affinity, which is probably due to its polarity. Class **IV** is very special as both polar RHS and lipophilic LHS contribute significantly to the intrinsic primary CCR8 potency as well as to the intrinsic potency at hERG. The increased importance of the lipophilic parts of compounds of this class in hERG binding is most likely caused by the fact that the majority of molecules in class **IV** possess two aromatic rings in their lipophilic LHS, consistent with structures of other CCR8 antagonists.[83]

Ranking Intrinsic hERG Binding Fragments. Intrinsic hERG binding fragments identified in the four classes are collected in Figure 8. The value shown next to the rank underneath of each fragment indicates the intrinsic hERG potency in logarithmic units calculated from the corresponding datapoint in Figure 7 as $\Delta x_i - \Delta y_i$. Contrary to current practice,[14–16] we recommend to avoid these molecular fragments not because they are lipophilic or carry a positive charge, but because they are found to be especially efficient in jeopardizing hERG selectivity within the particular structural classes. All of these fragments are located in the periphery of the molecules.

The vast majority of intrinsic hERG binding fragments detected (except for fragment **3** in class **IV** only) are polar, which suggests that a H-bonding network within the hERG

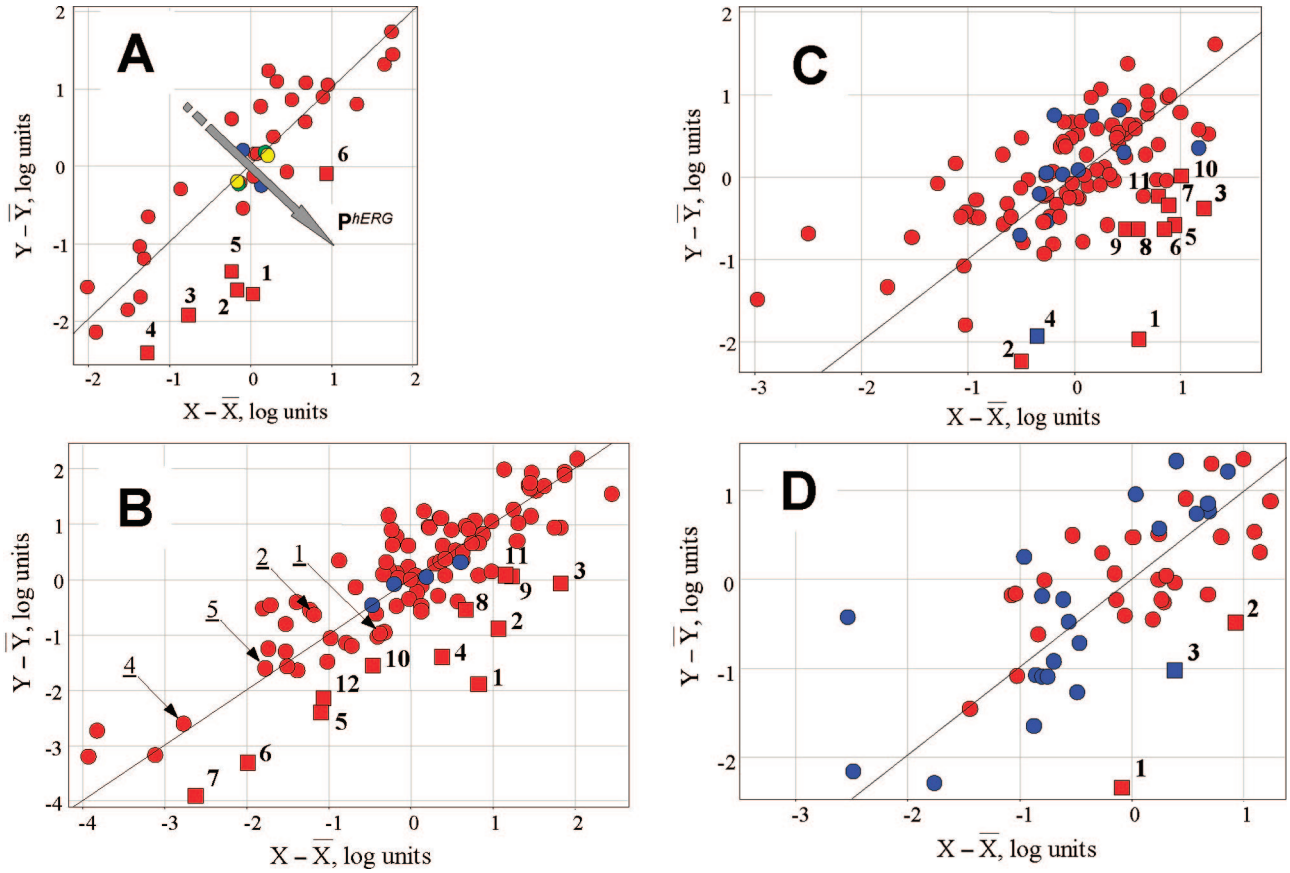

Figure 7. Detection of intrinsic hERG binding fragments in four classes of CCR antagonists by two-dimensional fragment-based QSAR analysis based on eq 2. Both coordinates, $X = pIC_{50}^{CCR} - \log D$, and $Y = pIC_{50}^{CCR} - pIC_{50}^{hERG}$, are centered. (A) class **I**; (B) class **II**; (C) class **III**; (D) class **IV**. Polar RHS fragments are shown in red; lipophilic LHS fragments or R^1, blue; R^2, green; R^3, yellow. Diagonal lines $\Delta X = \Delta Y$ designate average hERG lipophilicity baselines. The axis of intrinsic hERG potency, $P^{hERG} = pIC_{50}^{hERG} - \log D$, which is perpendicular to the hERG lipophilicity baseline, is indicated in (A). Consistent with eq 2, intrinsic hERG binding fragments designated by numbered squares are located below the average hERG lipophilicity baseline, whereas intrinsic hERG nonbinding fragments above the baseline. Numbers represent fragment ranks according to their contributions to intrinsic hERG potency of compounds of the given class. Fragments designated in (B) by underlined numbers are identical to those identified in class **I** as intrinsic hERG binding fragments.

channel represents a hallmark of intrinsic hERG potency. Most of the lipophilic fragments form hydrophobic interactions with the channel cavity and correspondingly contribute about as much to hERG potency as to compound lipophilicity. The fact that only one lipophilic intrinsic hERG binding fragment is identified in the four test series suggests that it does something very unusual in the hERG channel. The phenomenon of inherent binding propensity of particular lipophilic moieties of ligands has been well documented for a variety of targets[62,87,88] but not for hERG. An unusually high role of particular lipophilic groups in ligand binding affinity is believed to be caused by packing effects.[43] Distinct lipophilic groups, which participate in direct repulsive interactions with the hERG binding site, have been described in several structural classes.[9,85,86] To the best of our knowledge, we have identified the first lipophilic fragment that contributes to hERG potency much more (about 20-fold) than expected in line with its role in compound lipophilicity. Because the hERG channel binding site appears more flexible than other protein binding sites, it is unlikely that packing effects in the hERG channel can explain this effect.

Intrinsic hERG binding motifs are detected in particular structural classes, therefore the structure of the scaffold may be critical for activating those motifs. There are cases of a significant role of scaffolds in intrinsic hERG binding of peripheral fragments in the considered series. Four intrinsic hERG binding fragments identified in class **I** (**1**, **2**, **4**, and **5**) do not seem to have the same effect in class **II** (Figure 7B). Consistent with earlier findings, it is likely that the attachment topology of the peripheral fragments to the scaffolds may play a significant role in hERG binding.[7] Surprisingly, two pairs of identical intrinsic hERG binding motifs are identified in different structural classes, namely, fragment **3** in class **I** and **12** in class **II**, and fragment **10** in class **III** and **2** in class **IV**, which suggests that these especially potent hERG binding motifs are likely to have specific interactions within the hERG cavity, and the role of scaffolds can be secondary, probably because of their flexibility.

It is well documented that compounds carrying positive charges exhibit higher intrinsic propensities toward cationic ion channels than neutral ones.[25] Consistent with this observation, fragment **1** in class **III**, which carries a basic amine, the second positive charge in this molecule, shows especially high intrinsic propensity for the hERG channel. On the other hand, zwitterions are found to display lower hERG potencies than basic compounds taken at the same log*D* value.[25] This being the case, the average ability of acidic functions to decrease hERG binding affinity should be somewhat higher than the accompanied decrease of lipophilicity. Nevertheless, several intrinsic hERG binding moieties, namely, fragments **9** and **10** in class **II**, **5**–**11** in class **III**, and **2** in class **IV**, include acidic functions, which suggests that zwitterions per se do not represent a panacea for removing hERG binding in chemical series.

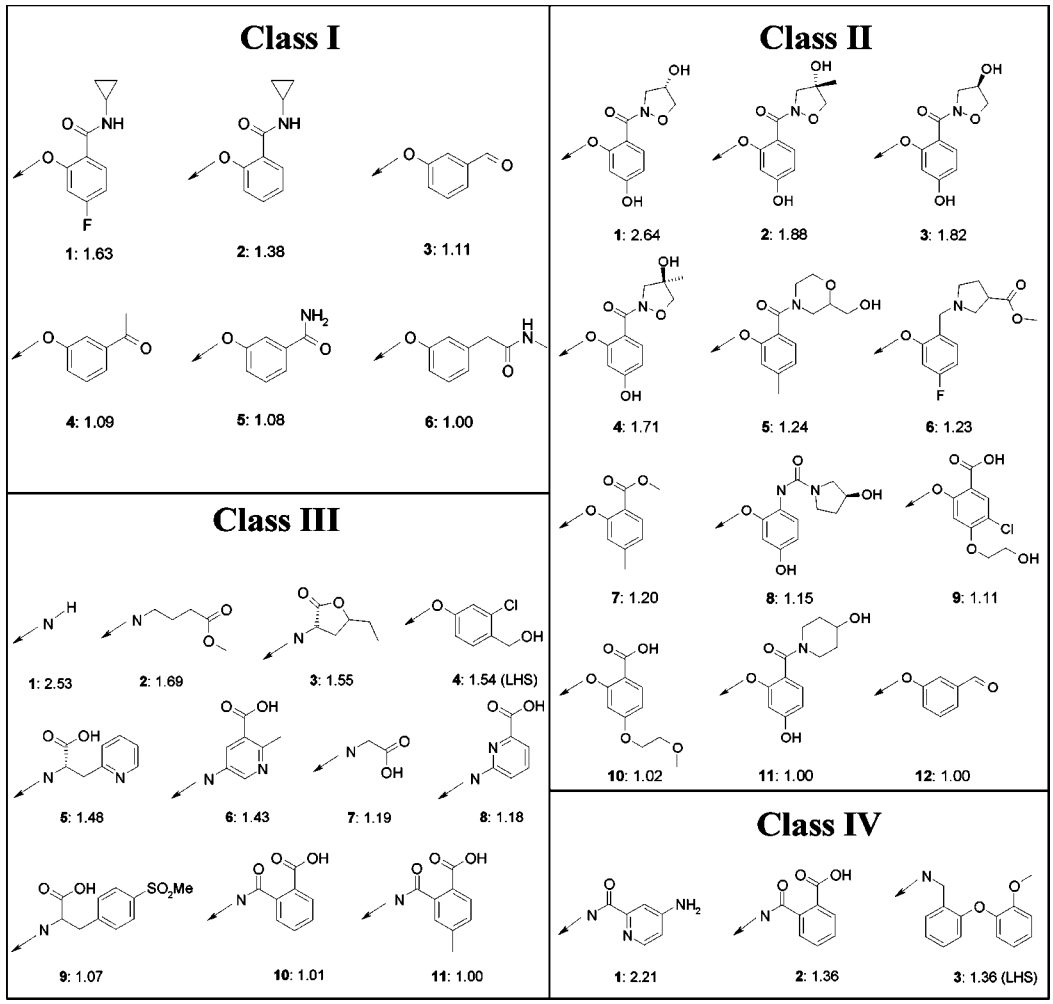

Figure 8. Structures of the intrinsic hERG binding motifs detected in the four test classes. Attachment atoms (amide functional group for class **IV**) are included and denoted by arrows. All fragments, except for **4** in class **III** and **3** in class **IV**, represent RHS of the molecules (Figure 4). Bold numbers designate ranks of the fragments in the particular class. The relative contribution of each fragment to intrinsic hERG potency of compounds (in logarithmic units) is given next to the rank. A cutoff value of one logarithmic unit is used. Each illustrated fragment is present once in a given class, except for **10** in class **III** (3 times), **2** in class **IV** (2 times), and **3** in class **IV** (18 times).

Repairing Peripheral Intrinsic hERG Binding Fragments. Figure 9 gives examples of subtle changes within these motifs, which are able to disrupt detrimental interactions with the hERG cavity. They include alkylation of basic secondary amine (fragment **1** in class **III**), reversing an amide (**2** in class **I**), removal of a H-bond donor (**1** and **9** in class **II**; **1** and **4** in class **III**; **1** in class **IV**), removal of a H-bond acceptor (**1** and **10** in class **II**; **5**, **6**, **8**, and **10** in class **III**), inverting a configuration of the chiral center carrying a polar group (**1** in class **II**), adding lipophilic groups (**3** in class **I**; **1** and **10** in class **II**; **2** in class **IV**), a change in topology (**10** in class **III**; **3** in class **IV**), changing the position of a polar atom (**1** in class **IV**), or replacing a polar group by a bioisostere (**2** in class **IV**). Most of these cases suggest that it is the accumulation of several polar functions on the periphery of a molecule that may turn the polar side into a motif capable of productive polar interactions with the hERG channel. This implies that cooperativity of nonhydrophobic interactions with hERG can play a crucial role in intrinsic hERG potency. The particular attachment topology, relative spatial locations, stereochemistry, and H-bonding donor/acceptor capacity of several peripheral polar groups are required for intrinsic hERG-binding propensity of these motifs, consistent with earlier observations.[7] Possible chemical alterations leading to reducing the intrinsic hERG-binding propensity of peripheral fragments identified in the test series appear to be the opposite to the conventional methods, which have been linked to reducing compound lipophilicity,[9,12,14–18,21,22,34] but in agreement with recent studies.[9] The solutions are to *remove* detrimental polar groups and/or *add* lipophilic groups and not the other way around. Small lipophilic groups added directly to polar intrinsic hERG binding motifs are likely to cause steric hindrances within hERG, thus disrupting the H-bonding network.

Obtained data indicate that carboxylic groups themselves are not the reason for the intrinsic hERG-binding propensities of most of the acidic motifs, as they can be repaired by removing adjacent heteroatoms, that is, fragments **9** and **10** in class **II** and fragments **5**, **6**, and **8** in class **III**. Nevertheless, in certain cases, acidic groups are capable of direct attractive interactions with the hERG channel. We found only one such case in the considered series, namely, fragment **10** in class **III**, which is also detected in class **IV** (fragment **2**; Figure 9). In this fragment, the carboxylic group is attached to the peripheral phenyl ring in the *ortho*-position leading to a V-shaped geometry, which is thought to be predisposed for hERG binding.[7] Summing up, zwitterions will have a guaranteed increased selectivity if the large decrease in lipophilicity associated with adding an acidic group to a basic scaffold is acceptable to the target protein, presumably by making a new strong compensating interaction not available to the hERG channel.[34]

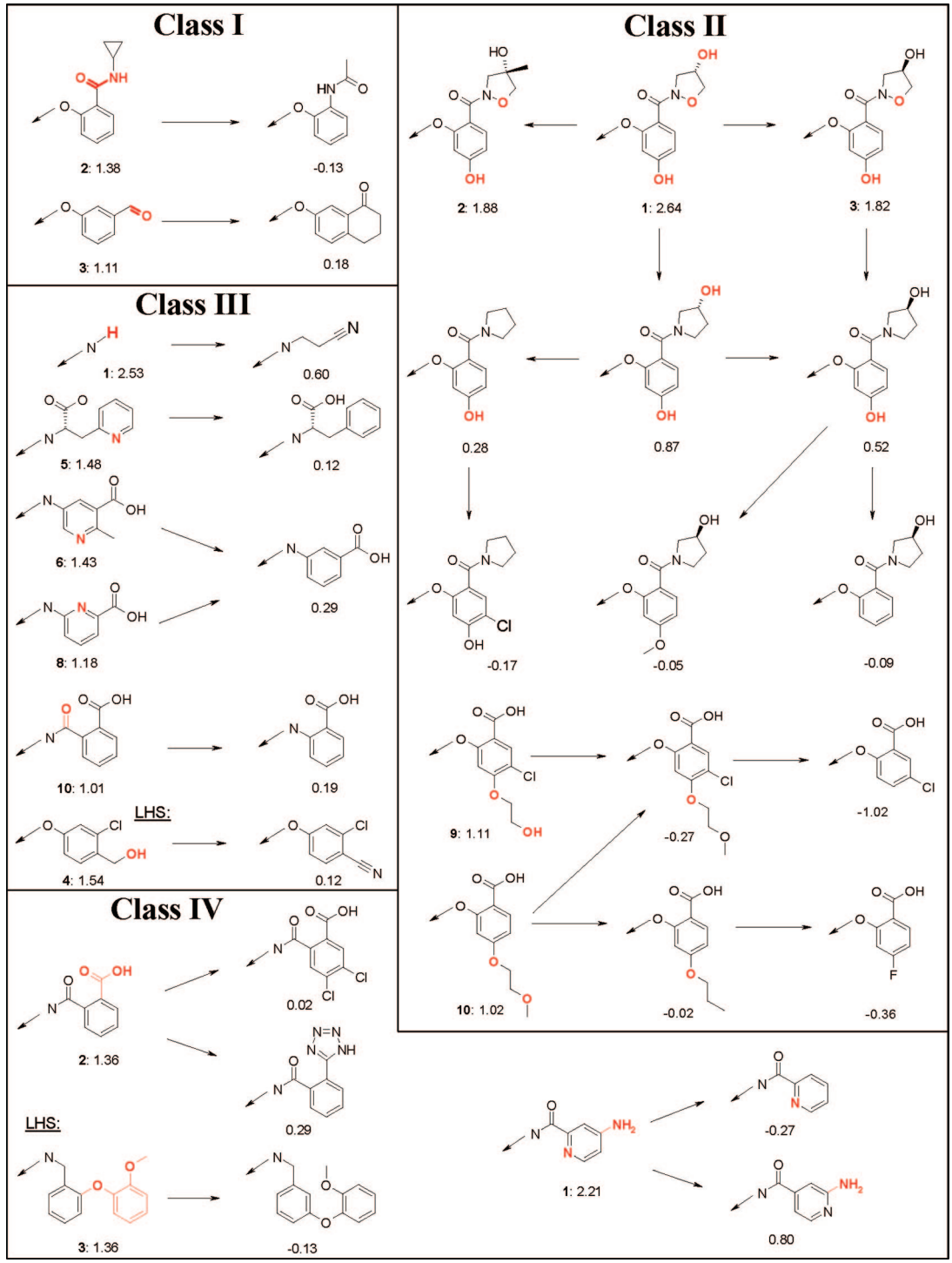

Figure 9. Structural changes within intrinsic hERG binding fragments that disrupt their productive intrinsic interactions with the hERG binding site. Functional groups, which potentiate the fragments and, hence, directly participate in attractive intrinsic hERG binding are shown in red. Bold numbers designate the ranks of fragments in the particular class. Indicated real values denote relative contributions of fragments to intrinsic hERG potency of compounds in this class. Fragments that correspond to the positive values decrease hERG selectivity of the corresponding compounds by making productive intrinsic interactions with the hERG channel.

The only lipophilic intrinsic hERG binding motif identified in the test series (fragment **3** in class **IV**) can be repaired by changes in the attachment topology from *ortho* to *meta*. The two aryl groups in fragment **3** are likely to be involved in multiple $\pi-\pi$ interactions with aromatic residues of the hERG channel. This case once again confirms the role of the *ortho*-substitution pattern for intrinsic hERG-binding propensity.[7]

Aryl groups and H-bond acceptors have been recognized as structural features of hERG blockers, which have high hERG-binding propensity.[1,7,17,22–24,39,66,89] Data presented in Figure 9 are consistent with these observations and further indicate that H-bond donors are also able to participate in H-bonding with the hERG channel binding site. It is seen that polar hydrogens of hydroxyls and amines are responsible for the high intrinsic hERG potency of fragments **1** and **9** in class **II** and fragment **1** in class **IV**. This suggests that, apart from the bifunctional hydroxyl groups of T623 and S624, which have been shown to be involved in H-bonding with polar functions of hERG

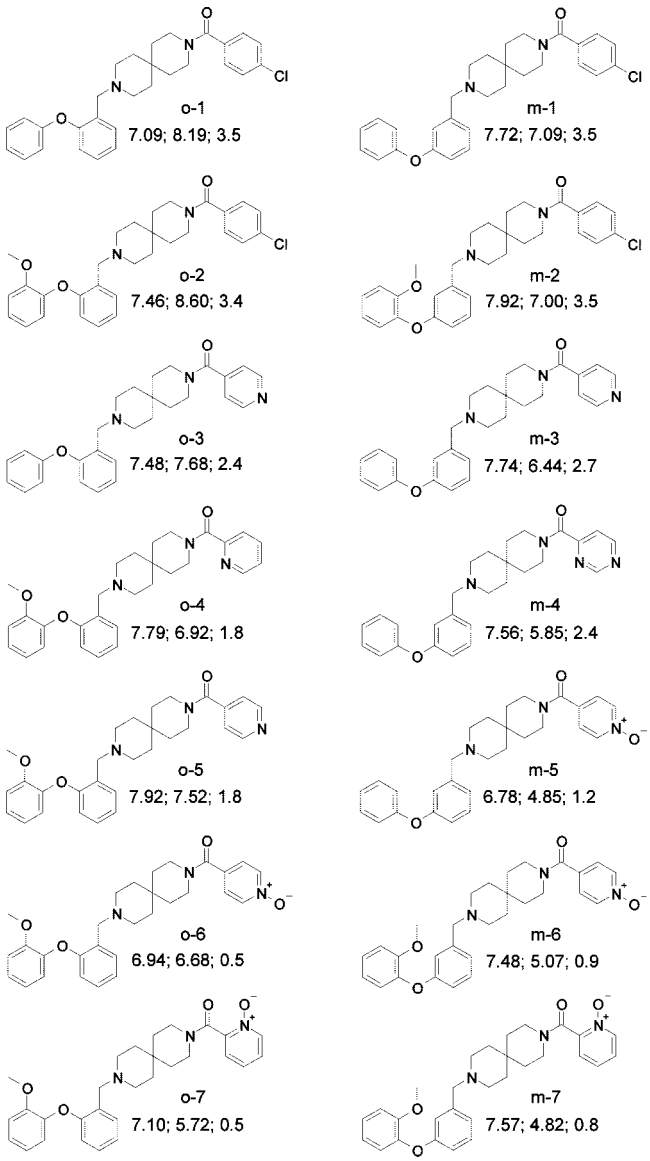

Figure 10. Structures of CCR8 antagonists of the class **IV**, which exemplify the strategy of overcoming hERG potency. Molecules with the *o*-phenoxyphenyl topology in the LHS are designated **o-1**−**o-7**. Molecules with the *m*-phenoxyphenyl topology in the LHS are designated **m-1**−**m-7**. The following three values are given for each compound: pIC_{50}^{CCR8}, pIC_{50}^{hERG}, and Log*D*.

blockers,[3,4,7,11,19] there might be other polar groups within the hERG channel cavity that are available for interactions with the enclosed hERG blockers and can function only as H-bond acceptors.

Jamieson et al.[9] have summarized successful examples of overcoming hERG binding and have formulated the discrete structural modifications (DSM) approach as one possible method of reducing hERG binding in chemical series. This approach urges subtle structural alterations in peripheral fragments of hERG blockers, not accompanied by significant changes in lipophilicity. The DSM approach is in line with one aspect of our strategy, targeted at disrupting direct attractive interactions with the hERG binding site.

Analysis of BLRs in Chemical Series To Steer Away from Undesirable Off-Target Binding. The value of BLRs in real life projects can be illustrated using a subset of 14 CCR8 antagonists of class **IV** (Figure 10). The subset is split into two groups by the structure of the lipophilic LHS. In the first group (**o-1** through **o-7**), compounds include the *o*-phenoxyphenyl

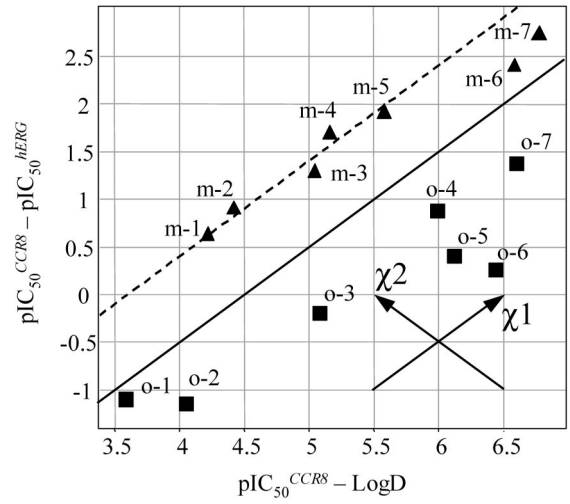

Figure 11. The plot of hERG selectivity (the left side of eq 2) vs lipophilicity-adjusted CCR8 potency (the first term of the right side of eq 2) of the compounds shown in Figure 10. Molecules with the *o*-phenoxyphenyl and *m*-phenoxyphenyl topology in the LHS are shown by squares and triangles, respectively. The solid line with the equation $pIC_{50}^{hERG} - LogD = 4.5$, represents a hERG lipophilicity baseline, which separates these groups. Changes along the axes $\chi 1$ and $\chi 2$ reflect improvements of hERG selectivity caused by the increase of the first and of the second terms of the right side of eq 2, respectively. The dashed line with the equation $pIC_{50}^{hERG} - LogD = 3.6$ approximates a lipophilicity-adjusted hERG potency of the most promising lead candidates.

moiety, whereas in the second group (**m-1** through **m-7**), the *ortho*-topology in the LHS is changed to *meta*-topology. Consistent with earlier findings,[7] the *ortho*-topology in the peripheral LHS inherent in the first group is identified to be the cause of the detrimental attractive nonhydrophobic interactions with the hERG channel (Figure 9). A significant role of lipophilicity in binding affinity to CCR8 and hERG can be seen when comparing the corresponding potencies of **o-2** and **o-6** or **m-2** and **m-6**. On the other hand, comparison of **o-1** and **o-3** or **m-1** and **m-3** may lead to the incorrect conclusion that compound lipophilicity drives hERG potency but not CCR8. The BLR approach clarifies the situation as it allows one to visualize intrinsic interactions with both the target and off-target binding sites, which represent the main driving force for selectivity.

Figure 11 depicts the hERG selectivity of compounds of the subset versus lipophilicity-adjusted CCR8 potency. The increase of polarity of compounds by replacing *p*-Cl-phenyl in the peripheral RHS by 2-pyridyl, 4-pyridyl, 2,4-pyrimidyl, 2-pyridyl-*N*-oxide, or 4-pyridyl-*N*-oxide leads to increasing hERG selectivity within each group roughly parallel to the hERG lipophilicity baseline, that is, along the $\chi 1$ axis. According to eq 2, this suggests that the polar functions in the RHS form H-bonds with the primary binding site, but are unable to do so in the hERG channel. Because intrinsic interactions with the hERG channel did not change, the compounds of each subclass tend to situate on the corresponding hERG lipophilicity baseline in Figure 11. This being the case, the resulting improvement of hERG selectivity has to be similar in the two groups because it is achieved only by decreasing hydrophobic interactions with the hERG channel, which is insensitive to structure and approximately equal to $\Delta LogD$, consistent with eq 1 at $a^{hERG} = 1$. Thus, it is not surprising that the difference in hERG selectivity that exists between the most lipophilic compounds of the groups, **o-1** and **m-1** (1.73 logarithmic units), remains about the same between the most polar compounds of these

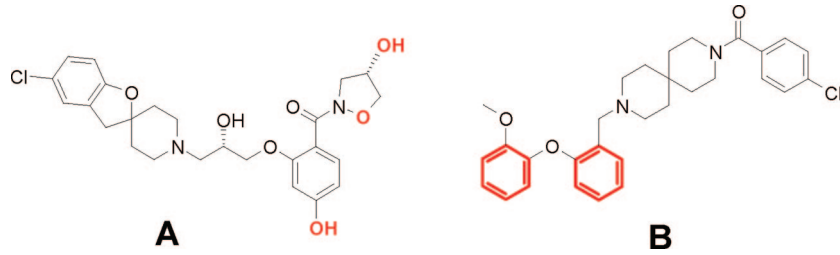

Figure 12. Structures of extreme cases of intrinsic hERG binders, which have been docked to the internal cavity of a hERG homology model. Experimental data: compound A, $pIC_{50}^{hERG} = 7.6$, log$D = 1.55$; compound B, $pIC_{50}^{hERG} = 8.6$, log$D = 3.4$. Functional groups, which are predicted to be directly involved in polar interactions with hERG residues, are shown in red.

groups, **o-7** and **m-7** (1.37 logarithmic units), although compound lipophilicity decreased considerably (by about three logarithmic units). The hERG lipophilicity baseline inherent in a particular structural subclass can be extrapolated to the required range of lipophilicity, and the resulting hERG selectivity of optimized compounds of a particular structural subclass can thus be predicted using the following expression

$$pIC_{50}^{CCR8} - pIC_{50}^{hERG} = pIC_{50}^{CCR8} - \text{Log}D - (pIC_{50}^{hERG} - \text{Log}D) \quad (4)$$

where the term in the parentheses quantifies the intrinsic interactions of compounds of a particular subclass with the hERG channel (eq 1). Setting the target values of pIC_{50}^{CCR8} and Log*D* to 8.5 and 1.5, respectively, and presuming that we will not be able to decrease the nondesolvation component of hERG potency within the subclass, the hERG selectivity of the target compound of the most promising **m**-subclass would be close to 3.4 logarithmic units (see the dashed line in Figure 11). This example illustrates the importance of a proper selection of the lead candidate with the highest potential for a subsequent hERG selectivity improvement in the course of lead optimization. All other factors being equal, the priority in the selection of the starting point has to be given to those candidates that exhibit the minimum of the lipophilicity-adjusted hERG potency, $pIC_{50}^{hERG} - \text{Log}D$.

Because compound lipophilicity can be decreased in the course of lead optimization only to a certain limit to maintain high compound bioavailability, in most cases, it is critical to further improve hERG selectivity without decreasing compound lipophilicity,[9] that is, to make structural alterations resulting in a progress in hERG selectivity along the $\chi 2$ axis (Figures 9 and 11). The suggested two-dimensional fragment-based QSAR analysis is able to rank particular molecular fragments in the given chemical series according to their ability to disrupt attractive intrinsic interactions with the hERG channel. In addition, the general rules of repairing peripheral intrinsic hERG binding fragments could be helpful. In the considered subclass, replacement of the intrinsic hERG binding fragment, *o*-(*o*-methoxyphenoxy)phenyl (fragment **3** in class **IV**, Figure 9), in the compound **o-2** by the fragment of similar lipophilicity results in the compound **m-2** with improved hERG selectivity (by 2.06 logarithmic units). The simplified subset consists of similar molecules to interpret the hERG selectivity progress in structural terms more easily. However, in real projects with thousands of structurally diverse compounds, the BLR-sensitive fragment-based QSAR analysis helps to detect favorable and detrimental fragments in directions of $\chi 1$ and $\chi 2$ and thereby direct lead optimization strategy in both directions more efficiently.

Docking of Intrinsic hERG Binders into a hERG Homology Model. Two hERG blockers (Figure 12) representing extreme cases of intrinsic hERG binding were docked into a homology model of the hERG channel. The purpose was to gain a structural hypothesis for the cooperative H-bonding (molecule **A**) or cooperative $\pi-\pi$ interactions (molecule **B**) as a plausible interpretation for intrinsic hERG binding. The predicted binding modes are illustrated in Figure 13. Despite the uncertainty of docking results in a homology model, and taking into account that each hERG blocker could have more than one binding mode in the hERG channel,[1] some characteristic features of putative binding modes can be ascertained. The intrinsic hERG binding peripheral moieties of both molecules are situated in the vestibule of the hERG channel, an unusually large central water-filled internal cavity located by the selectivity filter.[3,9,13,66,71,72] The lipophilic tails of both molecules are pointed toward the narrow intracellular opening of the inner helices.[22,66] Polar intrinsic hERG binding functions of molecule

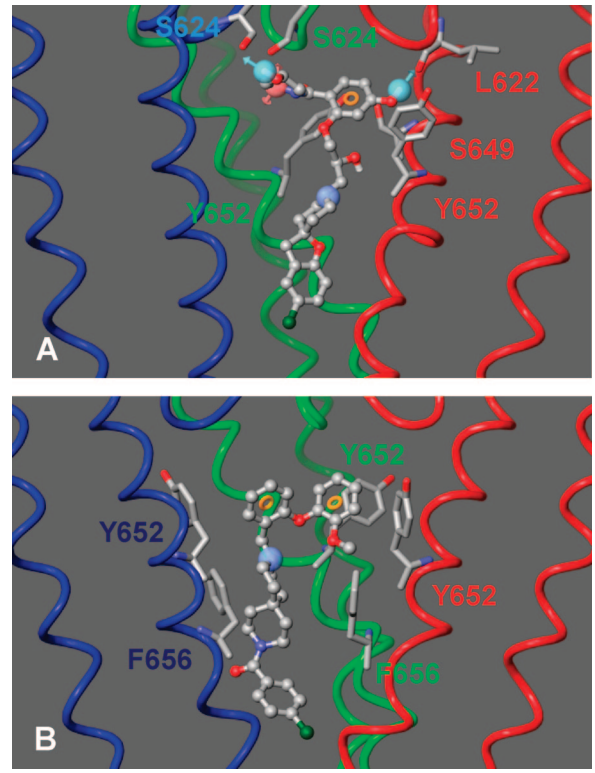

Figure 13. Putative binding modes of two extreme cases of intrinsic hERG binders in a homology model of hERG ion channel with highlighted pharmacophore features important for intrinsic interactions (Figure 9). Molecular structures of the hERG binders are given in Figure 12. (A) molecule **A**; (B) molecule **B**. One subunit of the tetrameric hERG channel models is removed for clarity of the views. Residues involved in direct attractive interactions with the intrinsic hERG binding fragments are illustrated. The pharmacophore features include H-bond donors (light blue spheres with arrows), a H-bond acceptor (pink sphere with an arrow), protonated nitrogen (dark blue sphere), and aryl groups (brown circles).

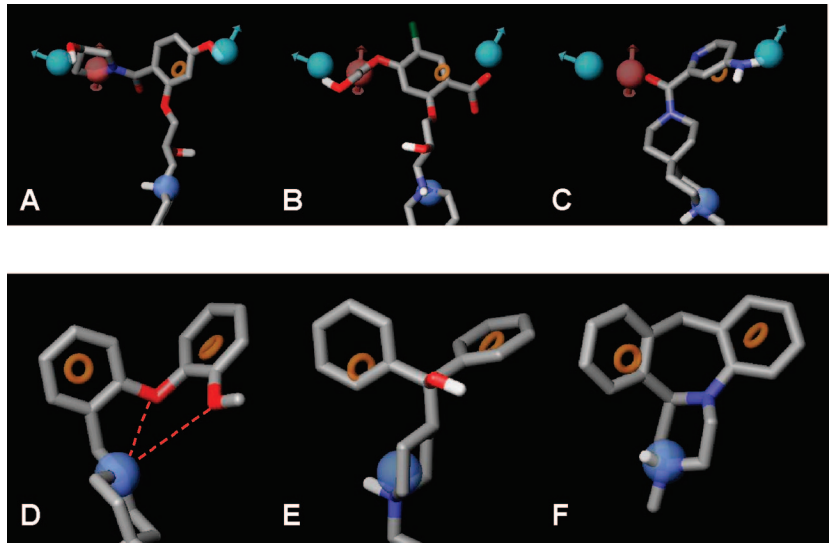

Figure 14. Two types of pharmacophore models for attractive intrinsic interactions with the hERG channel cavity, which describe structural features detrimental for hERG selectivity of CCR antagonists, mapped onto conformations of polar (A−C) and lipophilic intrinsic hERG binding fragments (D−F). The first pharmacophore (A−C) includes two H-bond donors (light blue sphere), one H-bond acceptor (pink sphere), one aryl group (brown torus), and a basic nitrogen (dark blue sphere). The second pharmacophore (D−F) includes two aryl groups and a basic nitrogen and represents a simplified form of Cavalli pharmacophore.[21] The following intrinsic hERG binding groups are mapped onto the pharmacophores: (A) fragment **1** from class **II**, (B) **9** from class **II**, (C) **1** from class **IV**, (D) **3** from class **IV**, (E) terfenadine, and (F) mianserin. The dotted lines in (D) denote intramolecular H-bonds.

A are likely to form multiple H-bonds within the hERG binding site (Figure 13A), whereas both aromatic rings of the intrinsic hERG binding fragment of molecule **B** could be involved in $\pi-\pi$ interactions with Y652 (Figure 13B). The majority of residues in the hERG channel directly interacting with these fragments in the obtained models are those known as critical for binding of many hERG blockers.[3,7,9,24,90] They include S624, Y652, and F656. Docking simulations further suggest that other residues can also be involved in intrinsic interactions of these particular hERG blockers, particularly the side chain of S649 and the backbone oxygen of L622.[24]

Pharmacophores for Attractive Intrinsic Interactions with hERG. The derived list of intrinsic hERG binding motifs (Figures 8 and 9) suggests that there are at least two likely hERG pharmacophores for intrinsic interactions, one for H-bonding, and the other for $\pi-\pi$ interactions. To capture spatial locations of the corresponding structural features of hERG blockers, we assigned pharmacophore features to the key functional groups of the two examples of intrinsic hERG binders taken in their docked conformations (Figure 13). The identified intrinsic hERG binding fragments from classes **I**−**IV** were split into two groups. The first group included all polar fragments, while the second group consisted of only fragment **3** detected in class **IV**. The latter group was augmented with known hERG blockers, which carry two aryl groups on one side of the basic nitrogen, namely, astemizole, clozapine, terfenadine, and mianserin. Conformations of intrinsic hERG binders were mapped onto the corresponding receptor-based hERG pharmacophores by the program Phase (Figures 13 and 14).

The first pharmacophore (Figures 13A and 14A−C) consists of a basic center, one aryl group, and a cluster of H-bonding features, including one acceptor and two donors. The separation of the H-bonding cluster from the basic center within this pharmacophore model is significantly larger than previously suggested (4–6 Å),[1] and ranges from 8.4 Å (for the acceptor) to 9.7 Å (for the most distant donor). This indicates that the ideal position of the basic center of hERG blockers within the hERG channel is quite elusive and that the possible locations of the positive charge resemble a cylinder, coaxial with the symmetry axis of the channel, rather than a sphere. The second pharmacophore (Figures 13B and 14D−F) consists of a basic center and two aryl groups, which are approximately equidistant from the basic center. The key feature of fragments that fit the first type of hERG pharmacophore is that they increase hERG potency by decreasing compound lipophilicity. The key feature of fragments matching the second type of hERG pharmacophore is that although they increase both hERG potency and compound lipophilicity, the amount of gained hERG potency considerably exceeds that expected from the gained lipophilicity.

The relative intrinsic potency of a ligand is thought to indicate the extent of enthalpic processes involved in ligand binding, such as H-bonding and $\pi-\pi$ interactions, and tends to represent the arithmetic sum of these contributions to the free energy of binding.[45] Using typical energy values for direct interactions with the binding site to be –0.9 kcal/mol for a $\pi-\pi$ interaction and between −1.0 and −2.5 kcal/mol for H-bonding,[43,45] we can inspect whether the intrinsic hERG potencies attributed to fragments **1** in class **II** and **3** in class **IV** (Figure 8) are consistent with the predicted binding modes in hERG (Figure 13). Assuming that the average hERG lipophilicity baseline is considered as a reference point of no interactions, the contribution of the polar peripheral moiety of molecule **A** to intrinsic hERG binding (2.64 logarithmic units or −3.6 kcal/mol) is equivalent to the energy of 1−4 H-bonds, which is consistent with the three H-bonds predicted by the QSAR analysis (Figure 9) and the model (Figure 13A). Similarly, the contribution of the lipophilic peripheral fragment of molecule **B** to its intrinsic hERG potency is 1.36 logarithmic units, which corresponds to an interaction energy of −1.86 kcal/mol and is indeed equivalent to the energy of two $\pi-\pi$ interactions.

The suggested strategy of overcoming hERG potency of preclinical compounds is based on measured values of potency and lipophilicity, Log$D_{7.4}$. Measured values of lipophilicity are widely used in the pharmaceutical industry because critical properties of drugs correlate with *n*-octanol/water partition coefficients, that is, permeability, solubility, binding to unrelated proteins, metabolic stability, clearance, and bioavailability. To design drugs, it is important to remain on experimental grounds

in lipophilicity estimations because this allows one to implicitly control these properties. Certainly, it would be of much help if we could replace measured values of lipophilicity with calculated predictions. Unfortunately, computational methods are still not good enough to completely replace measurements of lipophilicity. We tested the calculated values of ACDLog*D*7.4 and ACDLog*P* (ACDLabs version 8.00, Advanced Chemistry Development, Inc., Toronto, Canada) in the foregoing strategy, but the results were skewed. The obtained hERG lipophilicity baselines in the test series appeared too shallow, which contradicts experimental observations. Although the overall correlation of ACDLog*D* or ACDLog*P* with Log*D* values is normally rather high, in the considered classes, we found that the slopes of the Log*D*/ACDLog*D* and Log*D*/ACDLog*P* regressions are significantly below than 1. Besides, predictions of lipophilicity of unusual structures are usually poor, which jeopardizes the estimates of the hydrophobicity factors of the binding sites and, hence, the whole BLR approach. Therefore, at this point, we do not recommend using the calculated estimates of Log*D* in the BLR-dependent approaches for series of non-neutral compounds.

Conclusions

The large water-filled vestibule of the hERG channel offers a wealth of opportunities for attractive nondesolvation-related interactions with entrapped drug-like molecules. The interaction points within the hERG cavity are formed by such residues as S624, L622, Y652, and, possibly, T623 and S649. Because of the tetrameric structure of the hERG channel, these interaction points within the channel get multiplied by four and create an extensive network of functional groups within the cavity, which is capable of H-bonding or $\pi-\pi$ interactions with a variety of enclosed ligands,[2,66] especially when several polar or aryl functional groups are present at the periphery of the molecule. In this case, the peripheral moiety of the ligand is stabilized particularly well inside the hERG vestibule, which turns it into an intrinsic hERG binding fragment and dramatically decreases the hERG selectivity of the whole molecule. The rest of the hERG channel cavity represents a hydrophobic surface[22,66] that facilitates binding of lipophilic moieties of entrapped compounds due to structure-insensitive hydrophobic interactions.

To overcome problems of compounds associated with an undesirable inhibition of the hERG potassium ion channel most efficiently, we have outlined a new strategy that focuses on increasing the hERG selectivity of molecules instead of the common routine of decreasing hERG potency outside of the context of intended binding. This strategy highlights the importance of optimizing only direct enthalpic interactions with the intended target, while concomitantly reducing enthalpic interactions with the hERG binding site rather than considering the overall binding affinities. We have also identified several intrinsic hERG binding motifs, peripheral molecular fragments that bind to the hERG channel particularly efficiently and thereby may decrease hERG selectivity of compounds regardless of the primary target. The structure of the scaffold may be important for activating or inactivating these peripheral fragments.

The intrinsic hERG binding fragments should be ranked according to their contribution to the lipophilicity-adjusted or intrinsic hERG potency, $pIC_{50}^{hERG} - \log D$, rather than to the overall hERG potency, pIC_{50}^{hERG}. The top-ranked fragments possess lipophilicity-independent intrinsic hERG-binding propensity, and modeling suggests they are pointed toward the selectivity filter when bound to the hERG channel. These fragments have to be avoided or modified. The data suggest that simple changes in the peripheral intrinsic hERG binding motifs, for example, alkylation of the basic secondary amine, reversing an amide, removal of a H-bonding function, inverting a configuration of the chiral center carrying a polar group, adding lipophilic groups, alterations in topology, changing the position of a polar atom, or replacing a polar group by a bioisostere, may disrupt the detrimental interactions with the hERG channel vestibule cavity.

Overcoming selectivity issues in a chemical series is a very common task in drug design. Hereby we suggest a general strategy that can be applied in lead optimization programs to increase selectivity of compounds against nonspecific binding to target-unrelated hydrophobic binding sites. The strategy is based upon studies of BLRs of the undesired binding site for a compound series. We suggest using these relationships to avoid undesirable binding while retaining the intended potency. The strategy splits into two components. The first component is to decrease unwanted binding by engineering favorable polar interactions with the primary target. Because the polarity of a drug-like molecule can only be increased to a certain degree, the second component has to be used as well, which is to introduce subtle structural alterations leading to the disruption of attractive interactions, and the forming of repulsive interactions within the off-target binding site. It should be noted that this approach is inapplicable for selectivity issues of homologous proteins.

To successfully apply the BLR approach in chemical series to optimize the undesirable nonspecific hydrophobic binding, it is critical to utilize reliable estimates of compound lipophilicity. At this point we recommend using the measured values of $\text{Log}D_{7.4}$, at least for a series of charged compounds, although calculated predictions could be useful in the future as soon as they are in a better agreement with experimental estimates in a wide chemical space.

Experimental Section

The potency of binding of the compounds under consideration to chemokine receptors CCR1, CCR3, and CCR8 was measured in the corresponding binding assay described in the literature.[80,81b,d,91] The potency of binding to the hERG potassium ion channel was measured in an HEK cell line expressing recombinant hERG channel.[92,93] Measurements of compound lipophilicity, as described by the logarithm of the apparent *n*-octanol/water partition coefficient at pH = 7.4, $\text{Log}D_{7.4}$, are detailed in the literature.[94,95]

Acknowledgment. The authors gratefully acknowledge the support of many people at AstraZeneca R&D who have contributed to some aspects of the work presented in this paper. We particularly thank the Medicinal Chemistry teams at AstraZeneca Lund and AstraZeneca Charnwood who worked on the aforementioned chemokine projects and synthesized the compounds herein. We specifically express our gratitude to the following chemists of the CCR8 project chemistry team who synthesized the set of compounds exemplified in Figure 10: Lisa Alderin, Henrik Johansson, Anna Kristoffersson, Lena Ripa, and Marco Skrinjar. We are especially thankful to the Bioscience teams at both sites for biological experiments. We also thank Ramon Hendrickx for log*D* measurements and fruitful discussions. We thank Nicholas Tomkinson for writing a script for the QSAR analysis presented in the paper. We thank Niklas Blomberg for his homology model of the hERG potassium ion channel. Critical comments of Andy Davis, Jeff Morris, and Peter Kenny are greatly appreciated.

References

(1) Testai, L.; Bianucci, A. M.; Massarelli, I.; Breschi, M. C.; Martinotti, E.; Calderone, V. Torsadogenic cardiotoxicity of antipsychotic drugs: A structural feature, potentially involved in the interaction with cardiac hERG potassium channels. *Curr. Med. Chem.* **2004**, *11*, 2691–2706.

(2) Sanguinetti, M. C.; Tristani-Firouzi, M. hERG potassium channels and cardiac arrhythmia. *Nature* **2006**, *440*, 463–469.

(3) Stansfeld, P. J.; Sutcliffe, M. J.; Mitcheson, J. S. Molecular mechanisms for drug interactions with hERG that cause long QT syndrome. *Expert Opin. Drug Metab. Toxicol.* **2006**, *2*, 81–94.

(4) Recanatini, M.; Poluzzi, E.; Masetti, M.; Cavalli, A.; De Ponti, F. QT prolongation through hERG K^+ channel blockade: Current knowledge and strategies for the early prediction during drug development. *Med. Res. Rev.* **2005**, *25*, 133–166.

(5) Price, D. A.; Armour, D.; de Groot, M.; Leishman, D.; Napier, C.; Perros, M.; Stammen, B. L.; Wood, A. Overcoming hERG affinity in the discovery of the CCR5 antagonist maraviroc. *Bioorg. Med. Chem. Lett.* **2006**, *16*, 4633–4637.

(6) De Ponti, F.; Poluzzi, E.; Montanaro, N. Organizing evidence on QT prolongation and occurrence of *Torsades de Pointes* with non-antiarrhythmic drugs: A call for consensus. *Eur. J. Clin. Pharmacol.* **2001**, *57*, 185–209.

(7) Aronov, A. M. Predictive in silico modelling for hERG channel blockers. *Drug Discovery Today* **2005**, *10*, 149–155.

(8) Armer, R. E.; Morris, I. D. Trends in early drug safety. *Drug News Perspect.* **2004**, *17*, 143–148.

(9) Jamieson, C.; Moir, E. M.; Rankovic, Z.; Wishart, G. Medicinal chemistry of hERG optimizations: Highlights and hang-ups. *J. Med. Chem.* **2006**, *49*, 5029–5046.

(10) (a) Anonymous. *ICH S7B: The nonclinical evaluation of the potential for delayed ventricular repolarization (QT interval prolongation) by human pharmaceuticals*; European Medicines Agency: London, 2005; *25 May*, CPMP/ICH/423/02. (b) Anonymous. *ICH E14: The clinical evaluation of QT/QTc interval prolongation and proarrhythmic potential for non-antiarrhythmic drugs*; European Medicines Agency: London, 2005; *25 May*, CPMP/ICH/2/04.

(11) Mitcheson, J. S.; Chen, J.; Lin, M.; Culberson, C.; Sanguinetti, M. C. A structural basis for drug-induced long QT syndrome. *Proc. Natl. Acad. Sci. U.S.A.* **2000**, *97*, 12329–12333.

(12) Ekins, S.; Crumb, W. J.; Sarazan, R. D.; Wikel, J. H.; Wrighton, S. A. Three-dimensional quantitative structure-activity relationship for inhibition of human ether-a-go-go-related gene potassium channel. *J. Pharmacol. Exp. Ther.* **2002**, *301*, 427–434.

(13) Pearlstein, R.; Vaz, R.; Rampe, D. Understanding the structure-activity relationship of the human ether-a-go-go-related gene cardiac K^+ channel. A model for bad behavior. *J. Med. Chem.* **2003**, *46*, 2017–2022.

(14) Zolotoy, A. B.; Plouvier, B. P.; Beatch, G. B.; Hayes, E. S.; Wall, R. A.; Walker, M. J. A. Physicochemical determinants for drug induced blockade of hERG potassium channels: Effects of charge and charge shielding. *Curr. Med. Chem.* **2003**, *1*, 225–241.

(15) Bains, W.; Basman, A.; White, C. HERG binding specificity and binding site structure: evidence from a fragment-based evolutionary computing SAR study. *Prog. Biophys. Mol. Biol.* **2004**, *86*, 205–233.

(16) (a) Song, M.; Clark, M. Development and evaluation of an in silico model for hERG binding. *J. Chem. Inf. Model.* **2006**, *4*, 392–400. (b) Clark, M.; Song, M. Fragment based prediction of hERG binding. The 38th ACS Middle Atlantic Regional Meeting, Hershey, PA, June, 2006; MRM-520.

(17) Cianchetta, G.; Li, Y.; Kang, J.; Rampe, D.; Fravolini, A.; Cruciani, G.; Vaz, R. J. Predictive models for hERG potassium channel blockers. *Bioorg. Med. Chem. Lett.* **2005**, *15*, 3637–3642.

(18) Seierstad, M.; Agrafiotis, D. K. A QSAR model of hERG binding using a large, diverse, and internally consistent training set. *Chem. Biol. Drug Des.* **2006**, *67*, 284–296.

(19) Perry, M.; Stansfeld, P. J.; Leaney, J.; Wood, C.; de Groot, M. J.; Leishman, D.; Sutcliffe, M. J.; Mitcheson, J. S. Drug binding interactions in the inner cavity of hERG channels: Molecular insights from structure−activity relationships of clofilium and ibutilide analogs. *Mol. Pharmacol.* **2006**, *69*, 509–519.

(20) Morgan, T. K., Jr.; Sullivan, M. E. An overview of Class III electrophysiological agents: A new generation of antiarrhythmic therapy. *Prog. Med. Chem.* **1992**, *29*, 65–108.

(21) Cavalli, A.; Poluzzi, E.; De Ponti, F.; Recanatini, M. Toward a pharmacophore for drugs inducing the long QT syndrome: Insights from a CoMFA study of hERG K^+ channel blockers. *J. Med. Chem.* **2002**, *45*, 3844–3853.

(22) Aronov, A. M.; Goldman, B. B. A model for identifying hERG K^+ channel blockers. *Bioorg. Med. Chem.* **2004**, *12*, 2307–2315.

(23) Aronov, A. M. Common pharmacophores for uncharged human ether-a-go-go-related gene (hERG) blockers. *J. Med. Chem.* **2006**, *49*, 6917–6921.

(24) Österberg, F.; Åqvist, J. Exploring blocker binding to a homology model of the open hERG K^+ channel using docking and molecular dynamics methods. *FEBS Lett.* **2005**, *579*, 2939–2944.

(25) Waring, M. J.; Johnstone, C. A quantitative assessment of hERG liability as a function of lipophilicity. *Bioorg. Med. Chem. Lett.* **2007**, *17*, 1759–1764.

(26) Pearlstein, R. A.; Vaz, R. J.; Kang, J.; Chen, X.-L.; Preobrazhenskaya, M.; Shchekotikhin, A. E.; Korolev, A. M.; Lysenkova, L. N.; Miroshnikova, O. V.; Hendrix, J.; Rampe, D. Characterization of HERG potassium channel inhibition using CoMSiA 3D QSAR and homology modelling approaches. *Bioorg. Med. Chem. Lett.* **2003**, *13*, 1829–1835.

(27) Potet, F.; Bouyssou, T.; Escande, D.; Baró, I. Gastrointestinal prokinetic drugs have different affinity for the human cardiac human ether-à-gogo K^+ channel. *J. Pharmacol. Exp. Ther.* **2001**, *299*, 1007–1012.

(28) Rowley, M.; Hallett, D. J.; Goodcare, S.; Moyes, C.; Crawforth, J.; Sparey, T. J.; Patel, S.; Marwood, R.; Patel, S.; Thomas, S.; Hitzel, L.; O'Connor, D.; Szeto, N.; Castro, J. L.; Hutson, P. H.; MacLeod, A. M. 3-(4-Fluoropiperidin-3-yl)-2-phenylindoles as high affinity, selective, and orally bioavailable h5-HT_{2A} receptor antagonists. *J. Med. Chem.* **2001**, *44*, 1603–1614.

(29) Cooper, L. C.; Carlson, E. J.; Castro, J. L.; Chicchi, G. G.; Dinnell, K.; Di Salvo, J.; Elliott, J. M.; Hollingworth, G. J.; Kurtz, M. M.; Ridgill, M. P.; Rycroft, W.; Tsao, K. L.; Swain, C. J. 4,4-Disubstituted cyclohexylamine NK_1 receptor antagonists. II. *Bioorg. Med. Chem. Lett.* **2002**, *12*, 1759–1762.

(30) Scherer, C. R.; Lerche, C.; Decher, N.; Dennis, A. T.; Maier, P.; Ficker, E.; Busch, A. E.; Wollnik, B.; Steinmeyer, K. The antihistamine fexofenadine does not affect I_{Kr} currents in a case report of drug-induced cardiac arrhythmia. *Br. J. Pharmacol.* **2002**, *137*, 892–900.

(31) Fletcher, S. R.; Burkamp, F.; Blurton, P.; Cheng, S. K. F.; Clarkson, R.; O'Connor, D.; Spinks, D.; Tudge, M.; van Niel, M. B.; Patel, S.; Chapman, K.; Marwood, R.; Shepheard, S.; Bentley, G.; Cook, G. P.; Bristow, L. J.; Castro, J. L.; Hutson, P. H.; MacLeod, A. M. 4-(Phenylsulfonyl)piperidines: Novel, selective, bioavailable 5-HT_{2A} receptor antagonists. *J. Med. Chem.* **2002**, *45*, 492–503.

(32) Fraley, M. E.; Arrington, K. L.; Buser, C. A.; Cieko, P. A.; Coll, K. E.; Fernandez, C.; Hartman, G. D.; Hoffman, W. F.; Lynch, J. J.; McFall, R. C.; Rickert, K.; Singh, S.; Thomas, K. A.; Wong, B. K. Optimization of the indolyl quinoline class of KDR (VEGFR-2) kinase inhibitors: Effects of 5-amido- and 5-sulfonamido-indolyl groups on pharmacokinetics of hERG binding. *Bioorg. Med. Chem. Lett.* **2004**, *14*, 351–355.

(33) Fish, L. R.; Gilligan, M. T.; Humphries, A. C.; Ivarsson, M.; Ladduwahetti, T.; Merchant, K. J.; O'Connor, D.; Patel, S.; Philipps, E.; Vargas, H. M.; Hutson, P. H.; MacLeod, A. M. 4-Fluorosulfonylpiperidines: Selective 5-HT_{2A} ligands for the treatment of insomnia. *Bioorg. Med. Chem. Lett.* **2005**, *15*, 3665–3669.

(34) Zhu, B.-Y.; Jia, Z. J.; Zhang, P.; Su, T.; Huang, W.; Goldman, E.; Tumas, D.; Kadambi, V.; Eddy, P.; Sinha, U.; Scarborough, R. M.; Song, Y. Inhibitory effect of carboxylic acid group on hERG binding. *Bioorg. Med. Chem. Lett.* **2006**, *16*, 5507–5512.

(35) Springthorpe, B. hERG: One channel you don't want to tune in to!! *The 2nd Anglo-Swedish Medicinal Chemistry Symposium*, Åre, Sweden March, **2005**. (b) Springthorpe, B. The hERG channel: Tuned in? Chemical strategies for dialing out an off-target source of candidate failure. *The 232nd ACS National Meeting*; San Francisco, CA, September, 2006.

(36) Bell, I. M.; Gallicchio, S. N.; Abrams, M.; Beshore, D. C.; Buser, C. A.; Culberson, J. C.; Davide, J.; Ellis-Hutchings, N.; Fernandez, C.; Gibbs, J. B.; Graham, S. L.; Hartman, G. D.; Heimbrook, D. C.; Honmick, C. F.; Huff, J. R.; Kassahun, K.; Koblan, K. S.; Kohl, N. E.; Lobell, R. B.; Lynch, J. J.; Miller, P. A.; Omer, C. A.; Rodrigues, A. D.; Walsh, E. S.; Williams, T. M. Design and biological activity of (*S*)-4-(5-{[1-(3-chlorobenzyl)-2-oxopyrrolidin-3-ylamino]methyl}-imidazol-1-ylmethyl)benzonitrile, a 3-aminopyrrolidinone farnesyltrasferase inhibitor with excellent cell potency. *J. Med. Chem.* **2001**, *44*, 2933–2949.

(37) Friesen, R. W.; Ducharme, Y.; Ball, R. G.; Blouin, M.; Boulet, L.; Côté, B.; Frenette, R.; Girard, M.; Guay, D.; Huang, Z.; Jones, T. R.; Laliberté, F.; Lynch, J. J.; Mancini, J.; Martins, E.; Masson, P.; Muise, E.; Pon, D. J.; Siegl, P. K. S.; Styhler, A.; Tsou, N. N.; Turner, M. J.; Young, R. N.; Girard, Y. Optimization of a tertiary alcohol series of phosphodiesterase-4 (PDE4) inhibitors: Structure−activity relationship related to PDE4 inhibition and human ether-a-go-go related gene potassium channel binding affinity. *J. Med. Chem.* **2003**, *46*, 2413–2426.

(38) Vaz, R. J.; Gao, Z.; Pribish, J.; Chen, X.; Levell, J.; Davis, L.; Albert, E.; Brollo, M.; Ugolini, A.; Cramer, D. M.; Cairns, J.; Sides, K.; Liu, F.; Kwong, J.; Kang, J.; Rebello, S.; Elliot, M.; Lim, H.; Chellaraj, V.; Singleton, R. W.; Li, Y. Design of bivalent ligands using hydrogen bond linkers: Synthesis and evaluation of inhibitors of human β-tryptase. *Bioorg. Med. Chem. Lett.* **2004**, *14*, 6053–6056.

(39) Du, L.-P.; Tsai, K.-C.; Li, M.-Y.; You, Q.-D.; Xia, L. The pharmacophore hypothesis of I_{Kr} potassium channel blockers: Novel class III antiarrhythmic agents. *Bioorg. Med. Chem. Lett.* **2004**, *14*, 4771–4777.
(40) Kubinyi, H. Lipophilicity and drug activity. *Prog. Drug. Res.* **1979**, *23*, 97–198.
(41) Davis, A. M.; Dixon, J.; Logan, C. J.; Payling, D. W. Accelerating the progress of drug discovery. In *Pharmacokinetic challenges in drug discovery*; Pelkonen, O., Baumann, A., Reichel, A., Eds.; Springer: NY, 2002; pp 1–32,E. Schering Research Foundation, Workshop 37.
(42) Connolly, S.; Bennion, C.; Botterell, S.; Croshaw, P. J.; Hallam, C.; Hardy, K.; Hartopp, P.; Jackson, C. G.; King, S. J.; Lawrence, L.; Mete, A.; Murray, D.; Robinson, D. H.; Smith, G. M.; Stein, L.; Walters, I.; Wells, E.; Withnall, W. J. Design and synthesis of a novel and potent series of inhibitors of cytosolic phospholipase A_2 based on a 1,3-disubstituted propan-2-one skeleton. *J. Med. Chem.* **2002**, *45*, 1348–1362.
(43) Davis, A. M.; Teague, S. J. Hydrogen bonding, hydrophobic interactions, and failure of the rigid receptor hypothesis. *Angew. Chem., Int. Ed.* **1999**, *38*, 736–749.
(44) DeLano, W. L.; Ultsch, M. H.; de Vos, A. M.; Wells, J. A. Convergent solutions to binding at a protein−protein interface. *Science* **2000**, *287*, 1279–1283.
(45) Lewis, D. F. V.; Dickins, M. Baseline lipophilicity relationships in human cytochromes P450 associated with drug metabolism. *Drug Metab. Rev.* **2003**, *35*, 1–18.
(46) Lewis, D. F. V. Quantitative structure−activity relationships (QSARs) for substrates of human cytochromes P450 CYP2 family enzymes. *Toxicol. In Vitro* **2004**, *18*, 89–97.
(47) Lewis, D. F. V.; Jacobs, M. N.; Dickins, M. Compound lipophilicity for substructure binding to human P450s in drug metabolism. *Drug Discovery Today* **2004**, *9*, 530–537.
(48) Overton, E. *Studien über die Narkose, Zugleich ein Beitrag zur allgemeinen Pharmakologie*; Gustav Fischer: Jena, 1901; pp 1−195.
(49) Meyer, H. H. Theorie der Alkoholnarkose. *Arch. Exp. Pathol. Pharmakol.* **1899**, *42*, 109–118.
(50) Gao, Z.; Metz, W. A. Unraveling the chemistry of chemokine receptor ligands. *Chem. Rev.* **2003**, *103*, 3733–3752.
(51) Dragic, T.; Trkola, A.; Thompson, D. A. D.; Cormier, E. G.; Kajumo, F. A.; Maxwell, E.; Lin, S. W.; Ying, W.; Smith, S. O.; Sakmar, T. P.; Moore, J. P. A binding pocket for a small molecule inhibitor of HIV-1 entry within the transmembrane helices of CCR5. *Proc. Natl. Acad. Sci. U.S.A.* **2000**, *97*, 5639–5644.
(52) Westby, M.; van der Ryst, E. CCR5 antagonists: Host-targeted antivirals for the treatment of HIV infection. *Antiviral Chem. Chemother.* **2005**, *16*, 339–354.
(53) Horuk, R. BX471: A CCR1 antagonist with anti-inflammatory activity in man. *Mini-Rev. Med. Chem.* **2005**, *5*, 791–804.
(54) De Lucca, G. V. Recent developments in CCR3 antagonists. *Curr. Opin. Drug Discovery Dev.* **2006**, *9*, 516–524.
(55) Lien, E. J. C.; Hansch, C.; Anderson, S. M. Structure-activity correlations for antibacterial agents on gram-positive and gram-negative cells. *J. Med. Chem.* **1968**, *11*, 430–441.
(56) Seeman, P.; Roth, S.; Schneider, H. The membrane concentrations of alcohol anesthetics. *Biochim. Biophys. Acta* **1971**, *225*, 171–184.
(57) Kubinyi, H. 2D QSAR models: Hansch and Free-Wilson analyses. In *Computational Medicinal Chemistry for Drug Discovery*; Bultinck, P., De Winter, H., Langenaeker, W., Tollenaere, J. P., Eds.; Marcel Dekker: New York, Basel, 2004; pp 539–570.
(58) Rekker, R. F. The history of drug research: From Overton to Hansch. *Quant. Struct.-Act. Relat.* **1992**, *11*, 195–199.
(59) Ferguson, J. The use of chemical potentials as indices of toxicity. *Proc. R. Soc. London, Ser. B* **1939**, *B127*, 387–404.
(60) Hansch, C.; Zhang, L. Quantitative structure−activity relationships of cytochrome P-450. *Drug Metab. Rev.* **1993**, *25*, 1–48.
(61) Butora, G.; Morrielloo, G. J.; Kothandaraman, S.; Guiadeen, D.; Pasternak, A.; Parsons, W. H.; MacCoss, M.; Vicario, P. P.; Cascieri, M. A.; Yang, L. 4-Amino-2-alkyl-butyramides as small molecule CCR2 antagonists with favorable pharmacokinetic properties. *Bioorg. Med. Chem. Lett.* **2006**, *16*, 4715–4722.
(62) Bertagna, A. M.; Barrick, D. Nonspecific hydrophobic interactions stabilize an equilibrium intermediate of apomyoglobin at a key position within the AGH region. *Proc. Natl. Acad. Sci. U.S.A.* **2004**, *101*, 12514–12519.
(63) VanDer Kamp, K. A.; Qiang, D.; Aburub, A.; Wurster, D. E. Modified Langmuir-like model for modeling the adsorption from aqueous solutions by activated carbons. *Langmuir* **2005**, *21*, 217–224.
(64) Ruben, A. J.; Kiso, Y.; Freire, E. Overcoming roadblocks in lead optimization: a thermodynamic perspective. *Chem. Biol. Drug Des.* **2006**, *67*, 2–4.
(65) Free, S. M., Jr.; Wilson, J. W. A mathematical contribution to structure−activity studies. *J. Med. Chem.* **1964**, *7*, 395–399.
(66) Stansfeld, P. J.; Gedeck, P.; Gosling, M.; Cox, B.; Mitcheson, J. S.; Sutcliffe, M. J. Drug block of the hERG potassium channel: insight from modeling. *Proteins: Struct., Funct., Bioinformatics* **2007**, *68*, 568–580.
(67) Qiu, D.; Shenkin, P. S.; Hollinger, F. P.; Still, W. C. The GB/SA continuum model for solvation. A fast analytical method for the calculation of approximate Born radii. *J. Phys. Chem. A* **1997**, *101*, 3005–3014.
(68) Zhou, Y.; MacKinnon, R. The occupancy of ions in the K^+ selectivity filter: Charge balance and coupling of ion binding to a protein conformational change underlie high conduction rates. *J. Mol. Biol.* **2003**, *333*, 965–975.
(69) Ficker, E.; Jarolimek, W.; Brown, A. M. Molecular determinants of inactivation and dofetilide block in ether a-go-go (EAG) channels and EAG-related K^+ channels. *Mol. Pharmacol.* **2001**, *60*, 1343–1348.
(70) Kamiya, K.; Mitcheson, J. S.; Yasui, K.; Kodama, I.; Sanguinetti, M. C. Open channel block of hERG K^+ channels by vesnarinone. *Mol. Pharmacol.* **2001**, *60*, 244–253.
(71) Mitcheson, J. S.; Chen, J.; Sanguinetti, M. C. Trapping of a methanesulfonanilide by closure of the hERG potassium channel activation gate. *J. Gen. Physiol.* **2000**, *115*, 229–239.
(72) Mitcheson, J. S.; Perry, M. D. Molecular determinants of high-affinity drug binding to hERG channels. *Curr. Opin. Drug Discovery Dev.* **2003**, *6*, 667–674.
(73) Jiang, Y. X.; Lee, A.; Chen, J. Y.; Ruta, V.; Cadene, M.; Chait, B. T.; MacKinnon, R. X-ray structure of voltage-dependent K^+ channel. *Nature* **2003**, *423*, 33–41.
(74) Shealy, R. T.; Murphy, A. D.; Ramarathnam, R.; Jacobsson, E.; Subramaniam, S. Sequence-function analysis of the K^+-sensitive family of ion channels using a comprehensive alignment and the KcsA channel structure. *Biophys. J.* **2003**, *84*, 2929–2942.
(75) Jiang, Y.; Lee, A.; Chen, J.; Cadene, M.; Chait, B. T.; MacKinnon, R. The open pore conformation of potassium channels. *Nature* **2002**, *417*, 523–526.
(76) Friesner, R. A.; Banks, J. L.; Murphy, R. B.; Halgren, T. A.; Klicic, J. J.; Mainz, D. T.; Repasky, M. P.; Knoll, E. H.; Shelley, M.; Perry, J. K.; Shaw, D. E.; Francis, P.; Shenkin, P. S. Glide: A new approach for rapid, accurate docking and scoring. 1. Method and assessment of docking accuracy. *J. Med. Chem.* **2004**, *47*, 1739–1749.
(77) Halgren, T. A.; Murphy, R. B.; Friesner, R. A.; Beard, H. S.; Frye, L. L.; Pollard, W. T.; Banks, J. L. Glide: A new approach for rapid, accurate docking and scoring. 2. Enrichment factors in database screening. *J. Med. Chem.* **2004**, *47*, 1750–1759.
(78) (a) Bodkin, M.; Eriksson, T.; Hansen, P.; Hemmerling, M.; Henriksson, K.; Klingstedt, T.; Pettersson, L. Preparation of substituted 1-phenoxy-3-pyrrolidino(or piperidino)propan-2-ols as chemokine receptor modulators. *PCT Int. Appl.* WO2001062728, 2001, 191. (b) Eriksson, T.; Klingstedt, T.; Mussie, T. Preparation of substituted 1-benzyl-4-piperidinamines as chemokine receptor modulators. *PCT Int. Appl.* WO2001098273, 2001, 64.
(79) (a) Hossain, N.; Ivanova, S.; Mensonides-Harsema, M. Preparation of tricyclic spiropiperidines or spiropyrrolidines useful against disorders affected by modulation of chemokine receptors. *PCT Int. Appl.* WO2004005295, 2004, 281. (b) Hossain, N.; Ivanova, S. Preparation of tricyclic spiropiperidines as modulators of chemokine receptor activity. *PCT Int. Appl.* WO2005061499, 2005, 70. (c) Hossain, N.; Ivanova, S.; Mensonides-Harsema, M. Preparation of spiroheterocyclic-piperidine or -pyrrolidine derivatives as chemokine receptor modulators. *PCT Int. Appl.* WO2005054249, 2005, 54. (d) Baxter, A.; Hossain, N.; Ivanova, S.; Mensonides-Harsema, M.; Pimm, A.; Reuberson, J. Preparation of N-(3-phenoxy-2-hydroxypropyl)-tricyclic spiropiperidine derivatives as modulators of chemokine receptor activity. *PCT Int. Appl.* WO2005049620, 2005, 74.
(80) (a) Luckhurst, C.; Perry, M.; Springthorpe, B. Preparation of piperidine derivatives for use in the treatment of chemokine mediated disease states. *PCT Int. Appl.* WO2004029041, 2004, 72. (b) Luckhurst, C.; Perry, M.; Springthorpe, B. Preparation of piperidine derivatives for the treatment of chemokine or H1 mediated disease state. *PCT Int. Appl.* WO2004085423, 2004, 44. (c) Caffrey, M.; Luckhurst, C.; Mochel, T.; Perry, M.; Springthorpe, B. A preparation of (piperidinylmethyl)-piperidine derivatives, useful for the treatment of chemokine mediated diseases. *PCT Int. Appl.* WO2004087659, 2005, 67. (d) Luckhurst, C.; Mochel, T.; Perry, M.; Springthorpe, B.; Stein, L. Preparation of 1-aryl (aryloxy)- or (arylmethyl)-piperidinemethylpiperidines as histamine H1 receptor binding agents for treatment of chemokine-mediated diseases. *PCT Int. Appl.* WO2004099144, 2004, 72. (e) Mochel, T.; Perry, M.; Springthorpe, B. Preparation of piperidine derivatives for the treatment of chemokine mediated diseases. *PCT Int. Appl.* WO2005097775, 2005, 57.
(81) (a) Bladh, H.; Connolly, S.; Dyke, H. J.; Lisius, A.; Price, S.; Shamovsky, I.; Van den Heuvel, M. Preparation of novel diazaspiroalkanes and their use for treatment of chemokine receptor CCR8 mediated diseases. *PCT Int. Appl.* WO2005040167, 2005, 136. (b)

Connolly, S.; Skrinjar, M. Novel diazaspiroalkanes and their use for treatment of CCR8 mediated diseases. PCT Int. Appl. WO2006107252, 2006, 47. (c) Connolly, S.; Linnanen, T.; Skrinjar, M. Novel diazaspiroalkanes and their use for treatment of CCR8 mediated diseases. *PCT Int. Appl.* WO2006107253, 2006, 55. (d) Connolly, S.; Skrinjar, M. Novel diazaspiroalkanes and their use for treatment of CCR8 mediated diseases. *PCT Int. Appl.* WO2006107254, 2006, 44. (e) Börjesson, L.; Connolly, S.; Johansson, H.; Kristoffersson, A.; Linnanen, T.; Shamovsky, I.; Skrinjar, M. Preparation of novel diazaspiroalkanes for treatment of CCR8 mediated diseases. *PCT Int. Appl.* WO2007030061, 2007, 257.

(82) Clancy, C. E.; Kurokawa, J.; Tateyama, M.; Wehrens, X. H. T.; Kass, R. S. K^+ channel structure−activity relationships and mechanisms of drug-induced QT prolongation. *Annu. Rev. Pharmacol. Toxicol.* **2003**, *43*, 441–461.

(83) Ghosh, S.; Elder, A.; Guo, J.; Mani, U.; Patane, M.; Carson, K.; Ye, Q.; Bennett, R.; Chi, S.; Jenkins, T.; Guan, B.; Kolbeck, R.; Smith, S.; Zhang, C.; LaRosa, G.; Jaffee, B.; Yang, H.; Eddy, P.; Lu, C.; Uttamsingh, V.; Horlick, R.; Harriman, G.; Flynn, D. Design, synthesis, and progress toward optimization of potent small molecule antagonists of CC chemokine receptor 8 (CCR8). *J. Med. Chem.* **2006**, *49*, 2669–2672.

(84) McCauley, J. A.; Theberge, C. R.; Romano, J. J.; Billings, S. B.; Anderson, K. D.; Claremon, D. A.; Freidinger, R. M.; Bednar, R. A.; Mosser, S. D.; Gaul, S. L.; Connolly, T. M.; Condra, C. L.; Xia, M.; Cunningham, M. E.; Bednar, B.; Stump, G. L.; Lynch, J. J.; Macaulay, A.; Wafford, K. A.; Koblan, K. S.; Liverton, N. J. NR2B-selective *N*-Methyl-D-aspartate antagonists: Synthesis and evaluation of 5-substituted benzimidazoles. *J. Med. Chem.* **2004**, *47*, 2089–2096.

(85) Blum, C. A.; Zheng, X.; De Lombaert, S. Design, synthesis, and biological evaluation of substituted 2-cyclohexyl-4-phenyl-1*H*-imidazoles: Potent and selective neuropeptide Y Y5-receptor antagonists. *J. Med. Chem.* **2004**, *47*, 2318–2325.

(86) Kim, D.; Wang, L.; Hale, J. J.; Lynch, C. L.; Budhu, R. J.; MacCoss, M.; Mills, S. G.; Malkowitz, L.; Gould, S. L.; Demartino, J. A.; Springer, M. S.; Hazuda, D.; Miller, M.; Kessler, J.; Hrin, R. C.; Carver, G.; Carella, A.; Henry, K.; Lineberger, J.; Schleif, W. A.; Emini, E. A. Potent 1,3,4-trisubstituted pyrrolidine CCR5 receptor antagonists: effects of fused heterocycles on antiviral activity and pharmacokinetic properties. *Bioorg. Med. Chem. Lett.* **2005**, *15*, 2129–2134.

(87) Dorovska, V. N.; Varfolomeev, S. D.; Kazanskaya, N. F.; Klesov, A. A.; Martinek, K. Influence of the geometric properties of the active center on the specificity of α-chymotrypsin catalysis. *FEBS Lett.* **1972**, *23*, 122–124.

(88) Fersht, A. R.; Shindler, J. S.; Tsui, W.-C. Probing the limits of protein-amino acid side chain recognition with the aminoacyl-tRNA synthetases. Discrimination against phenylalanine by tyrosyl-tRNA synthetases. *Biochemistry* **1980**, *19*, 5520–5524.

(89) Choe, H.; Nah, K. H.; Lee, S. N.; Lee, H. S.; Lee, H. S.; Jo, S. H.; Leem, C. H.; Jang, Y. J. A novel hypothesis for the binding mode of HERG channel blockers. *Biochem. Biophys. Res. Commun.* **2006**, *344*, 72–78.

(90) Fernandez, D.; Ghanta, A.; Kauffman, G. W.; Sanguinetti, M. C. Physicochemical features of the hERG channel drug binding site. *J. Biol. Chem.* **2004**, *279*, 10120–10127.

(91) Needham, M.; Sturgess, N.; Cerillo, G.; Green, I.; Warburton, H.; Wilson, R.; Martin, L.; Barratt, D.; Anderson, M.; Reilly, C.; Hollis, M. Monocyte chemoattractant protein-1: Receptor interactions and calcium signaling mechanisms. *J. Leukocyte Biol.* **1996**, *60*, 793–803.

(92) Springthorpe, B.; Strandlund, G. Radiolabeled bispidine compound and assay for I_{Kr} potassium channel blocking activity. *PCT Int. Appl.* WO2005037052, 2005, 22.

(93) Murphy, S. M.; Palmer, M.; Poole, M. F.; Padegimas, L.; Hunady, K.; Danzig, J.; Gill, S.; Gill, R.; Ting, A.; Sherf, B.; Brunden, K.; Stricker-Krongrad, A. Evaluation of functional and binding assays in cells expressing either recombinant or endogenous hERG channel. *J. Pharmacol. Toxicol. Methods* **2006**, *54*, 42–55.

(94) Donovan, S. F.; Pescatore, M. C. Method for measuring the logarithm of the octanol-water partition coefficient by using short octadecyl-poly(vinyl alcohol) high-performance liquid chromatography columns. *J. Chromatogr., A* **2002**, *952*, 47–61.

(95) Box, K.; Elliott, S.; Cimpan, G. High throughput pK_a and log*D*7.4 measurements. *PharmaChem* **2003**, *2*, 55–59.

JM070543K